I.O.S.

WAVES RECORDED OFF KINNAIRDS HEAD

BY
K.L. THORNE & R. GLEASON

REPORT NO. 226
1986

NATURAL ENVIRONMENT RESEARCH COUNCIL

INSTITUTE OF
OCEANOGRAPHIC
SCIENCES

INSTITUTE OF OCEANOGRAPHIC SCIENCES

Wormley, Godalming, Surrey, GU8 5UB.

(042 - 879 - 4141)

(Director: Dr A.S. Laughton FRS)

Bidston Observatory,

Birkenhead, Merseyside, L43 7RA.

(051 - 653 - 8633)

When citing this document in a bibliography the reference should be given as follows:-

THORNE, K.L. & GLEASON, R. 1986 Waves recorded off Kinnairds Head. Data for February 1980 to January 1982 at position 57° 55'N, 001° 54'W. Summary analysis and interpretation report. *Institute of Oceanographic Sciences, Report*, No. 226, 69pp.

INSTITUTE OF OCEANOGRAPHIC SCIENCES

BIDSTON

Waves recorded off Kinnairds Head

Data for February 1980 to January 1982
at position 57° 55'N, 001° 54'W

Summary analysis and interpretation report

by

K.L. Thorne & R. Gleason*

I.O.S. Report No. 226

1986

The preparation of this report and the collection of the data contained in it have been financed by the Department of Energy

* *Present address:*

47 Birch Close
Corfe Mullen
Wimborne
DORSET

CONTENTS

LIST OF FIGURES

1. INTRODUCTION

1.1 Site description

The site at which the wave measurements were taken is shown on the map in figure 1.1. The buoy was moored in a water depth of approximately 88 metres at position 57°55.8'N,001°54.1'W. It is about 26 kilometres NNE of Kinnairds Head, Banffshire, NE Scotland.
The receiving site was on Quarry Head, about 3 kilometres SW of Rosehearty, Banffshire.

1.2 Description of measuring and recording systems

Wave measurements were made using a standard Waverider buoy moored as described by Humphery (1982). This instrument senses the vertical acceleration of the buoy by means of a stabilized accelerometer and uses analogue double integrators to reconstitute the surface elevation. This information is transmitted ashore via a high frequency (HF) radio link employing a frequency modulated (FM) subcarrier to encode the wave height information.
At Quarry Head the buoy's transmissions were received and a counting arrangement (described in Appendix I) was used to decode the wave height information. In this way a measure of surface elevation was obtained at 0.5 second intervals in the form of a digital count. This was recorded on magnetic tape using a Microdata digital data logger. The time between successive records was 3 hours, and the length of each record was 17 minutes. A back-up cassette system was also employed to log the FM buoy-signal directly. These cassettes could be used to provide in-fill data in the event of a malfunction of the Microdata.

1.3 Calibration and maintenance

The buoy was maintained on site by Wimpey Laboratories Ltd (now Wimpol Ltd) under contract to IOS. Regular replacement visits were made by Wimpey Laboratories Ltd and, in addition, special buoy-replacement visits were also made either when data reception stopped, or when data quality fell below acceptable standards. Appendix IV contains a brief history of the site.
The buoys were calibrated periodically by Wimpey Laboratories Ltd staff using the facilities at the National Maritime Institute at Hythe. Buoy sensitivity has been found in practice to be within ± 2%, and the decoding technique described in Appendix I has reduced variations in sensitivity due to the shore station equipment to a negligible value. Therefore the overall sensitivity of the system is stable to within ± 2%. A local site agent changed the Microdata cartridges, cassette tapes and also reported signal-loss and any other malfunctions.

1.4 Wave data coverage and return (figures 1.4 (a) - 1.4 (f))

The data covered the period from 1 February 1980 to 31 January 1982. For this period 2470 of the 5848 possible Microdata records were either missing or classified invalid, resulting in a data return of 57.76%. No attempt has been made to correct any bias which may have resulted from missing/invalid records, because of the uncertain reliability of the available techniques.

	Month Number											
YEAR	1	2	3	4	5	6	7	8	9	10	11	12
1980	--	38	155	163	149	27	50	242	42	11	69	--
1981	182	215	215	139	189	31	168	234	216	213	216	235
1982	179											
TOTAL	361	253	370	302	338	58	218	476	258	224	285	235

TABLE 1.4 : Number of valid records for each calendar month , with totals for the whole period.

(However, there is one exception: simple gap-filling by linear interpolation, up to a maximum of 7 consecutive records, has been carried out for the purpose of persistence calculations only: see section 3.6)
It can be seen from table 1.4 that there was a poor representation for the month of June and that August had a good data return. Although there is little seasonal bias, the data return over the two year period was generally poor. The approximate times when missing/invalid records occurred may be derived from the plots in figure 1.4 which shows Hs as a time series. On these plots each vertical line represents a valid record, and the height of the line is proportional to the value of Hs for that record; therefore these plots also indicate the variation of Hs with time.

2. WIND DATA - COMPARISON WITH THE LONG-TERM AVERAGE

This section is intended to place the wind speeds recorded during the wave data gathering period into context, by relating them to the long term wind speed results. It is intended that this information should allow a qualitative assessment of how typical the measured waves are of the longer time scale. The meteorological station nearest to the wave measurement site is Fraserburgh ($57^{o}40'N$, $002^{o}00'W$). The data used are hourly winds speeds from February 1970 to January 1982.

2.1 Monthly variation of wind speeds (figure 2.1)

Mean wind speeds for each of the calendar months of the two year period of this report are plotted. (Data for November 1980 were unavailable). In addition, the 'long-term' mean wind speed and its standard deviation are calculated and plotted for each of the twelve calendar months. Comparing monthly means for the 'long-term' data with that from the years when wave data were recorded, it can be seen that the wind speeds in winter were slightly higher than the long-term mean: in most months at least one of the two year values lies above the standard deviation. In summer the wind speeds are slightly lower than the long-term mean, though all values lie within the standard deviation.

2.2 Yearly variation of wind speeds (figure 2.2)
The year-to-year variability of wind conditions is illustrated in this figure. It shows, for each year, the maximum value of wind speed, the means of the next N highest wind speeds, where N = 5, 10, 20, 50, 100 (thus the highest 186 wind speeds are represented) and the overall mean wind speed.
It can be seen that for 1973/4 and 1981/2 the maximum wind speeds are higher than those recorded for any of the other years, whilst the overall mean wind speeds for these same years are consistent with the general trend during the twelve year period. The 1981/2 maximum which is the larger of those mentioned above (seen on figure 2.2) occurred during the period for which wave measurements are available, between 23rd November 1981 at 2100hrs and 24th November 1981 at 0001hrs; when wind conditions were 53 knots 270^{o} and 56 knots 280^{o} respectively. Under these circumstances the wave conditions at Kinnairds Head are fetch-limited, and consequently this storm did not generate the highest waves recorded during the report period (see section 3 for highest wave).

3. WAVE DATA - DESCRIPTION AND DISCUSSION OF THE PRESENTATIONS
Where figures show seasonal data, the seasons are defined as follows:

Summer - April to September
Winter - October to March

The maximum value of Hs in these two years of data was recorded on the 28th February 1981 at 1500hrs. Wind conditions on this day were near gale force, South Easterlies. There was an increase in wind speed during the latter part of the day, yielding a mean wind speed of 29.5 knots. Under these circumstances the wave conditions at Kinnairds Head are not fetch-limited and a Hs value of 8.65 metres was recorded; the associated value of Tz is 9.70 seconds and of Hmax(50) is 16.29 metres.

3.1 Statistics of variations of wave heights

3.1.1 Monthly variation of Hs (figure 3.1.1)
For each month, the mean significant wave height is calculated and plotted seperately for each year. The yearly variation is most pronounced for the months February and September, with the greatest variation in September.

3.1.2 Yearly variation of Hs (figure 3.1.2)
The year-to-year variability of wave conditions is illustrated in this figure. It shows, for each year, the maximum value, the means of the next N highest values where N = 5, 10, 20, 50, 100 (thus the highest 186 values of Hs are represented) and the overall mean value of Hs. The plot shows that the overall mean wave conditions are similar for each of

the two years, and that the maximum Hs value for 1981/2 is larger than that for 1980/1.

3.2 Statistics of wave heights

3.2.1 Occurrence of Hs (figures 3.2.1.1 - 3.2.1.3)

The percentage occurrence of Hs is shown by means of histograms. It can be seen from figure 3.2.1.3 that approximately 76% of the annual Hs occurrences lie between 0.5 and 2.5 metres.

3.2.2 Exceedance of Hs and Hmax(3hr) (figures 3.2.2.1. - 3.2.2.3.)

These graphs may be used to estimate the fraction of the time during which Hs is greater than or less than, a given height. For instance, from figure 3.2.2.2 it may be seen that during the winter the significant wave height exceeded 4 metres for approximately 6% of the time.

3.3 Design wave heights

The methods used to calculate the design wave height (the most probable height of the highest wave with a return period of 50 years) are described in Appendix III. The results obtained by different methods are given below:

3.3.1 Weibull distribution of Hs (figure 3.3.1)

The parameters of the Weibull distribution which most closely fits the data are A = 0.62 metres, B = 1.13 metres and C = 1.07. This distribution is represented by the straight line in figure 3.3.1 Extrapolation of this line to a return period of 50 years yields a value of Hs of 12.2 metres. The value of Tz associated with this Hs is approximately 11.8 seconds, resulting in a value of the design wave height of 22.7 metres.

3.3.2 Fisher-Tippett I distribution of Hs (figure 3.3.2)

The parameters of the Fisher-Tippett I distribution which most closely fit the data are a = 1.06 metre^{-1} and b = 1.14. This distribution is represented by the solid straight line on figure 3.3.2.
However, inspection of the plotted points suggests that the data falls on two approximately straight line segments: one extending up to 6 metres and one above 6 metres. The latter segment which includes the top 6 classes of the sample distribution contains only 10 observations out of a total of 3378 and is thus poorly defined. In spite of this, it is these observations which are most relevant to the problem of estimating extreme waves and we cannot disregard the information contained in them. With these considerations in mind we construct two further (dashed) lines L1 and L2 which give the best fit (by eye) to the two segments. Extrapolation of each of the resulting three lines to a return period of 50 years gives, for line L1 a value of Hs(50) of 11.0, for line L2 a value of Hs(50) of 13.4, and for the best fit line a value of Hs(50) of 12.3 metres. The approximate values of Tz associated with each of these values of Hs are 11.1, 12.4, and 11.8 seconds respectively. Using these figures the design wave height (Hmax(50)) for each of these lines are 20.5, 24.8 and 22.8 metres respectively. The range of these values, about 4.3 metres, can be taken as the uncertainty

in the design wave prediction introduced by the extrapolation process and is essentially due to the poor sampling of the higher waves. Hmax(50) is thus 22.8 ± 2.3 metres using the Fisher-Tippett I distribution as our model.

3.3.3 Individual Wave Model (figure 3.3.3)
The value of steepness used by the wave-by-wave method of determining the design wave height (as described in Appendix III) is 1:13 and the inverse mean period is 0.20 Hz. Using these values and the Fisher-Tippett I parameters given in section 3.3.2, the data which appear in figure 3.3.3 are obtained; by interpolation the design wave height is found to be 25.1 metres. A higher value of design wave height is expected from this method than from the two methods described above, for reasons stated in Appendix III.

3.4 Statistics of wave periods
The percentage occurrences of each of three wave period parameters (Tz, Tbar, and Te) are shown on a series of histograms.

3.4.1 Occurrence of Tz (figures 3.4.1.1 - 3.4.1.3)
In figure 3.4.1.3 the most frequently occurring values of Tz in the data set lie between 4.0 and 4.5 seconds (17.2% of the total). All values of Tz lie between 2.5 and 10.0 seconds.

3.4.2 Occurrence of Tbar (figures 3.4.2.1 - 3.4.2.3)
In figure 3.4.2.3. the most frequently occurring values of Tbar in the data set lie between 4.5 and 5.0 seconds (14.6% of the total). All values of Tbar lie between 2.5 and 11.5 seconds.

3.4.3 Occurrence of Te (figures 3.4.3.1 - 3.4.3.3)
In figure 3.4.3.3 the most frequently occurring values of Te in the data set lie between 5.5 and 6.0 seconds (12.4% of the total). All values of Te lie between 3.0 and 13.0 seconds.

3.5 Statistics of wave height and period combined.
These figures (sometimes called 'scatter' plots) show the numbers of wave records having particular combinations of values of Hs and period parameters (Tz, Tbar, and Te). The numbers of wave records are presented as parts per thousand (the total number of valid observations being shown on each figure), except for those which would be less than one part per thousand; these are shown instead as single occurrences and are distinguished by being underlined.

3.5.1 Occurrences of Hs and Tz combined (figures 3.5.1.1 - 3.5.1.3)
On these figures points of equal occurrences are joined by contour lines to give an indication of the bivariate probability distribution of Hs and Tz, and to illustrate the correlation between them. A wave 'steepness' (as defined in Appendix III) can be calculated for each (Hs,Tz) pair. A line is drawn on figure 3.5.1.3 showing a 'steepness' of 1:12, which is the limiting 'steepness' for the main body of the data. (Wave 'steepness' as shown in this figure are less than the maximum of 1:7 for an individual wave, since Hs and Tz are parameters

averaged over a number of waves most of which have 'steepness' less than this maximum).

3.5.2 Occurrences of Hs and Tbar combined (figures 3.5.2.1. - 3.5.2.3)
These figures show data boundaries similar to those of wave 'steepness' in figures 3.5.1.1 to 3.5.1.3.

3.5.3 Occurrences of Hs and Te combined (figures 3.5.3.1 - 3.5.3.3)
On these figures lines of constant wave power per unit length of wave crest are shown (in Kw/m), using the formula applicable to deep water (see Appendix II). It should be noted that using the deep water formula instead of the depth-dependent formula results in an underestimate of wave power; the magnitude of this underestimate depend on the depth of the water and on the form of the spectrum. Typically for this site, the underestimation is less than 5%.

3.6 Presentation of persistence of calms and of storms of Hs
Seasonal presentations of persistence of calms and of storms of Hs are omitted, because of the lack of continuity of the data (figures 1.4(A) - 1.4(F) illustrate this). The two year period of wave data is presented in figures 3.6.1 and 3.6.2.

3.6.1 Persistence of calms of Hs (Figure 3.6.1)
Information about, for example, calms of Hs less than 1.0 metre can be derived from this figure. The mean duration of calms was approximately 28 hours (with a standard deviation of 34 hours); and the time occupied by these events was 28% of the total observation time (given on the figure as 11643 hours). To calculate the number of such events which are likely to occur in a complete year, we proceed as follows, assuming that the statistics of our incomplete data set are representative of those of a typical complete year.
The number of hours in a complete year = 24 x 365 = 8760, and so Hs is less than 1.0 metre for 28% x 8760 = 2453 hours. The number of events is time period/mean duration of each event = 2453/28 = 88 events per year.

3.6.2 Persistence of storms of Hs (figure 3.6.2)
Similar information can be obtained for storms. Information about, for example, storms of Hs greater than 4.0 metres can be derived from this figure. The mean duration of storms was approximately 14 hours (with a standard deviation of 15 hours); and the time occupied by these events was 4% of the total observation time (given on the figure as 11643hours). To calculate the number of such events which are likely to occur in a complete year, we proceed as above, assuming that the statistics of our incomplete data set are representative of those of a typical complete year.
The number of hours in a complete year = 24 x 365 = 8760 and so Hs is greater than 4.0 metres for 4% x 8760 = 350 hours. The number of events is time period/mean duratuion of each event = 350/14 = 25 events per year.

3.7 Distribution of wave energy with Hs and Te. (figures 3.7.1 - 3.7.3)
For each wave record the wave power (P) per metre of wave crest is calculated from Hs and Te using the formula applicable to deep water. (see Appendix II and the note in section 3.5.3) The total energy flux at the buoy position during the period T is given by:

$$E = \int_0^T P(t)dt$$

which is in kWh/m provided t is measured in hours.

We approximate this, assuming P remains constant over the interval between records by:

$$\Delta t \sum_i P_i$$

where i is the observation index,
Δt is the observation interval and is equal to 3 hours for this site,
P is the power, and the sum is over the total number of 3-hourly observations in period T, thus for a single 3-hourly period the energy = $P\Delta t$.

For each class of (Hs,Te) the energy from all records with Hs and Te values falling within the class is summed. The total energy within each class is then expressed in parts per thousand of the overall total energy and is presented in these figures (a zero indicates less than one part per thousand). In figure 3.7.3 it can be seen that a large proportion of the wave energy measured at the site during this two year period is associated with values of Hs and Te in the middle sector of their ranges.

3.8 Occurrence of Qp (figures 3.8.1 - 3.8.3)
For each record Qp, which is proportional to the degree of peakedness of the spectrum, is calculated (see Appendix II). The most frequently occurring values of Qp in the data set lie between 1.5 and 2.5 (approximately 61.0%). All values of Qp lie between 0.5 and 5.5 (figure 3.8.1.3).

4 ACKNOWLEDGEMENTS
Contributions have been made towards the collection, analysis and presentation of the Kinnairds Head wave data by several members of the Applied Wave Research Group and of the Instrument Engineering Group, both based at the Taunton laboratory of the Institute of Oceanographic Sciences. Thanks are due to the Meteorological Office for supplying the wind data.

5 REFERENCES

HUMPHERY J. D. 1982. Operational experiences with Waverider buoys and their moorings.
Institute of Oceanographic Sciences
Report No 145.

APPENDIX I

Frequency logging of wave data

The Waverider buoy employs a 259Hz frequency modulated (FM) subcarrier to encode wave height information and has a nominal calibration so that an upward motion of the buoy of 1 metre displacement results in an increase in subcarrier frequency by 1.86Hz. Traditionally the wave height information is extracted from the signal by monitoring the V.C.O. (voltage control oscillator) voltage in a phase locked loop demodulator. In the IOS system however a different approach is used. The 259Hz FM signal is applied to a phase locked loop which multiplies the subcarrier frequency by a factor of 128 and also serves to filter out any extraneous noise. The phase locked loop output is subtracted from a signal with a fixed frequency of 128 x 290Hz. This gives a signal whose frequency depends upon wave height and for which (290-259) x 128Hz corresponds to zero wave height. The frequency of this signal is counted over a period of one half second, so that for the zero wave height a count of 1984 is obtained. In the presence of waves the count will change by -1.86 x 64 counts per metre of upward displacement.

The counting scheme described above determines the frequency response of the detector system which has the form:

$$\frac{\sin x}{x}$$

where $x = \pi ft$, t is the time period over which the frequency is counted (0.5 seconds); and f is the sea wave frequency. For high frequencies (above 1Hz) the response function should be slightly modified to take account of the frequency response inherent in the phase locked loop.

This system has two advantages over the traditional analogue logging system: Firstly, the receiver and demodulator do not require regular calibration. Secondly, the system frequency response serves as a precisely defined low pass anti-alias filter.

APPENDIX II

Method of spectral analysis and derivations of wave parameters

The digital time-series of water surface elevations (recorded for approximately 17 minutes with a sampling interval of 0.5 seconds) allows an estimate to be made of the spectrum of the sea for the three-hour period over which the time-series is considered to be representative. An outline of the method of spectral analysis used is given below.

II.1 The Fast Fourier Transform

Using the Fourier theorem, the elevation of the sea surface above its mean at time t is given by

$$h(t) = \sum_{i=1}^{\infty} \left\{ a_i \cos \frac{2\pi i t}{T} + b_i \sin \frac{2\pi i t}{T} \right\}$$

where

$$a_i = \frac{2}{T} \int_0^T h(t) \cos \frac{2\pi i t}{T} \, dt$$

$$b_i = \frac{2}{T} \int_0^T h(t) \sin \frac{2\pi i t}{T} \, dt$$

T is the record length.

The Fast Fourier Transform, based on the above relationships, is used to compute the pairs of coefficients, a_i and b_i, at the fundamental frequency

$$f_0 = \frac{1}{T}$$

and at integral multiples of this frequency up to the Nyquist frequency

$$f_{max} = \frac{1}{2\Delta T}$$

where ΔT is the sampling interval.
The sample estimate of the spectrum at the ith frequency, Φ_i, is then computed as

$$\Phi_i = \frac{1}{2f_0} (a_i^2 + b_i^2) .$$

II.2 Tapering of the data

Variance of the wave record which is not located at one of the harmonic frequencies appears in the spectral estimates not only of the harmonics adjacent to the true frequency but in a band of harmonics. This 'leakage' leads to biassed estimates in that on balance a small proportion of the variance which should appear in the neighbourhood of the spectral peak 'leaks' towards higher and lower frequencies. The effect can be reduced by tapering the ends of the time-series data smoothly to zero before performing the Fast Fourier Transform; a

'cosine taper' applied to 12.5% of the record at each end has been used on the data described in this report. (This leads to a small increase in the sampling errors of the spectral estimate.)

II.3 Smoothing the spectral estimates

The spectral estimates, Φ_i, have a standard error of 100%. This large standard error may be reduced by taking the average of consecutive spectral estimates, and assigning to it the mid-frequency of the band of estimates used. Some of the data used in this report are derived from smoothed spectral estimates, S_j, which have been averaged in blocks of ten.

$$S_j = \frac{1}{10} \sum_{i=10j-9}^{10j} \Phi_i$$

and

$$f_j = (10j - 4.5) f_0.$$

II.4 Application to the wave data

The wave data described in this report are derived from time-series containing 2048 values of sea surface elevation taken at 0.5 second intervals.

Therefore $$f_0 = \frac{1}{2048} \text{ Hz} = .0009766 \text{ Hz}$$

and $$f_{max} = 1 \text{ Hz}.$$

Smoothing the spectral estimates in blocks of ten results in 102 smoothed estimates at the following frequencies

$$f_1 = .00537 \text{ Hz}$$

$$f_{max} = .992 \text{ Hz}$$

$$\Delta f = .009766 \text{ Hz}.$$

The normalised standard error of the smoothed spectral estimates is 32%, although the tapering process increases this error by a small amount.

II.5 Definition of spectral moments

The nth moment of a continuous spectrum is

$$m_n = \int_0^\infty f^n E(f)\, df$$

where $E(f)$ is the spectral density at frequency f.

For the discrete spectra produced from the digital time-series, the following equation has been used in the calculation of the spectral moments.

$$m_n = \frac{1}{T} \sum_{i=i_L}^{i_U} f_i{}^n \Phi_i$$

where $i_L = 42$; ($f_{42} = .0410$Hz),
$i_U = 651$; ($f_{651} = .6357$Hz).

II.6 Derivation of wave parameters

The wave parameters presented in this report are derived from the spectral moments using the following identities.

$$Hs = 4\sqrt{m_0}$$

$$Tz = \sqrt{\frac{m_0}{m_2}}$$

$$\overline{T}\ (Tbar) = \frac{m_0}{m_1}$$

$$Te = \frac{m_{-1}}{m_0}\ .$$

The spectral peakedness parameter Qp (GODA(1970)) is computed from

$$Qp = \frac{2\sum_{j=j_L}^{j_U}(f_j S_j^2)}{T m_0^2}$$

where $j_L = 5$; ($f_5 = .0444$Hz)
$j_U = 65$; ($f_{65} = .6304$Hz)
(It should be noted that the smoothed spectral estimates are used in the calculation of the peakedness parameter.)

Wave power may be calculated from the spectra using the expression

$$P = \int E(f)\, V_g(f,d)\, df$$

where V_g is the group velocity at frequency f and in water of depth d. An approximation to this expression has been used in this report, based on the assumption that the wave measurements were made in deep water: in this case

$$V_g(f,d) = V_g(f) = \frac{g}{4\pi f}$$

which leads to

$$P' = 0.49\, Hs^2\, Te$$

where P' is in kilowatts per metre of wave crest
Hs is in metres
Te is in seconds.

II.7 Reference

GODA Y 1970. Numerical experiments on wave statistics with spectral simulation. Report of the Port and Harbour Research Institute 9, No 3, 3-57.

APPENDIX III

Details of methods used for calculating design wave heights

III.1 By finding the long-term distribution of Hs

III.1.1 Hs is used as a measure of the "sea-state" (i.e. the intensity of wave activity), and it is sampled every 3 hours. It is assumed that a set of Hs data for one year, or an integral number of years, is representative of the wave climate.
For each value of Hs, the probability that this value will not be exceeded is calculated; this probability is then plotted against Hs. The axes are scaled according to an extreme-value distribution, so that data with a perfect fit would appear as a straight line on the diagram. This procedure is carried out using extreme-value distributions defined in the following ways

Weibull

$$\text{Prob}(Hs \leq h) = \begin{cases} 1 - \exp\left[-\left(\frac{h-A}{B}\right)^C\right], & \text{for } h > A \\ 0, & \text{for } h \leq A \end{cases}$$

where B and C are positive, and A represents a lower bound on h.

Fisher-Tippett I (first asymptote)

$$\text{Prob}(Hs \leq h) = \exp\left[-\exp(-ah+b)\right]. \qquad a > 0$$

Fisher-Tippett III (third asymptote)

$$\text{Prob}(Hs \leq h) = \begin{cases} \exp\left[-\left(\frac{A-h}{B}\right)^C\right], & \text{for } h \leq A \\ 1, & \text{for } h > A \end{cases}$$

where B and C are positive, and A represents an upper bound on h. (See FISHER AND TIPPETT(1928) and GUMBEL (1958) for the derivations of these distributions.)

For each extreme-value distribution the best-fit straight line is drawn; this line is then extrapolated to the desired probability (see section III.1.2) and the corresponding value of Hs is read off as the "design sea-state".

III.1.2 To calculate the "sea-state" which will be exceeded only once in N years, a storm duration of D hours needs to be assumed. The probability that a randomly chosen time will be within this storm is then

$$\frac{D}{24 \times 365.25 \times N}$$

IOS uses D = 3 hours (this choice is discussed in section III.1.5) which gives

$$\text{Probability} = \frac{3.422 \times 10^{-4}}{N}$$

$$= 6.845 \times 10^{-6} \quad \text{for} \quad N = 50 \text{ years}$$

III.1.3 The value of Tz for the "design sea-state" is required before the highest wave in the storm can be calculated. This is derived from the bivariate distribution of Hs and Tz (figure 3.5.1.3). A line is drawn across this at the "design sea-state" value of Hs and the most likely value of Tz (the modal value) is then estimated using extrapolations of the probability contours.

III.1.4 The most probable value of the highest zero-up-cross wave in the storm is then derived by assuming that the heights of such waves follow a Rayleigh distribution whose probability density function is

$$\text{prob}(h) = \frac{2h}{(Hrms)^2} \exp\left[-\left(\frac{h}{Hrms}\right)^2\right]$$

where $Hrms \approx \frac{Hs}{\sqrt{2}}$.

Exact theory is not available for zero-up-cross wave heights, but this distribution has been found to be an adequate fit to measured data. If there are n waves in the recording interval (3hr), then the probability that the highest wave, H, in three hours is less than h is

$$\text{Prob}(H \leq h) = \left\{1 - \exp\left[-\left(\frac{h}{Hrms}\right)^2\right]\right\}^n$$

with a corresponding probability density function

$$\frac{2n}{(Hrms)^2} h \exp\left[-\left(\frac{h}{Hrms}\right)^2\right]\left\{1 - \exp\left[-\left(\frac{h}{Hrms}\right)^2\right]\right\}^{n-1}$$

The most probable value (the mode) of this probability density function is usually used and is given by

$$Hmax(3hr) = Hrms\sqrt{\Psi}$$

where Ψ is a function of Tz which may be found using either figure 7 or equation 6.1-2 in TANN(1976).

III.1.5 In choosing the value of storm duration D, it should be noted that the effect of increasing D is to decrease the value of Hs for a given return period N. However, it also increases the ratio of Hmax(3hr) to Hs. It is found that in practice these effects roughly cancel and typically the value of Hmax(3hr) changes by only 3 per cent for a change of D from 3 to 15 hours. The choice of D is therefore not critical.

Many details of the above procedures may be found in TANN(1976).

III.2 By a wave-by-wave method

III.2.1 BATTJES(1970) shows that the probability that a randomly chosen wave will have a height H greater than h is

$$\text{Prob}(H>h) = \frac{\int_0^\infty \int_0^\infty R(h,Hs)\, Tz^{-1}\, p(Tz,Hs)\, dHs\, dTz}{\int_0^\infty \int_0^\infty Tz^{-1}\, p(Tz,Hs)\, dHs\, dTz} \quad \ldots\ldots\ldots\ldots\ldots\ldots (1)$$

where $R(h,Hs)$ is the Rayleigh cumulative probability function and $p(Tz,Hs)$ is the joint probability density function of Hs and Tz.

III.2.2 TANN makes the following suggestion in an unpublished manuscript. In order that values of Hs higher than those actually measured may be represented in the calculation of this probability, the values of Hs are assumed to have a long-term cumulative probability function $F(Hs)$, and a probability density function $f(Hs) = F'(Hs)$.

For each value of Hs throughout the long-term distribution, an average value of Tz^{-1} is used (denoted by $\overline{Tz^{-1}(Hs)}$). It is defined as

$$\overline{Tz^{-1}(Hs)} = \int_0^\infty Tz^{-1}\, \frac{p(Tz,Hs)}{f(Hs)}\, dTz$$

Therefore

$$\int_0^\infty Tz^{-1}\, p(Tz,Hs)\, dTz = \overline{Tz^{-1}(Hs)}\, f(Hs)$$

which, when substituted into equation (1), allows the probability of exceedance to be written

$$\text{Prob}\,(H>h) = \frac{\int_0^\infty R(h,Hs)\, \overline{Tz^{-1}(Hs)}\, f(Hs)\, dHs}{\int_0^\infty \overline{Tz^{-1}(Hs)}\, f(Hs)\, dHs} .$$

The value of $\overline{Tz^{-1}(Hs)}$ used with each value of Hs is chosen to satisfy the condition of constant wave "steepness", where the relationship between "steepness"(1:s), water depth(d), Hs and Tz is

$$Tz = \sqrt{\frac{2\pi s Hs}{g}\, \coth\left(\frac{2\pi d}{sHs}\right)} .$$

The value for the steepness used in this report is given in section 3.3.3.
The long-term distribution used in the computation for this report is the Fisher-Tippett I extreme-value distribution, whose probability density function is

$$f(Hs) = a \exp\left[(b - aHs) - \exp(b - aHs)\right]$$

The constants a,b are determined graphically as described in section III.1.1, and their values as used in this report are given in section 3.3.2.

III.2.3 Thus the probability of a wave exceeding each particular wave height may be found, and this probability may be converted into a return period of N years using the formula

$$N = \frac{1}{365.25 \times 24 \times 3600 \times \overline{T}^{-1} \times Prob}$$

where $\overline{T}^{-1} = \text{average}\left(\frac{1}{\text{period}}\right)$.

The value of the average wave period is contained in section 3.3.3. Since $\overline{T}^{-1}$ is a non-analytic function of Prob, the simplest way of solving the problem is to calculate Prob for various values of h, calculate N for each of these values of Prob, and then interpolate to find the height h corresponding to the required value of N(in this case 50 years).

Whereas the method described in section III.1 assumes that the highest wave in a 50-year period will come from the most stormy 3-hour period in 50 years, the individual wave method takes into account the probability that storms other than the highest may provide the wave with a 50-year return period. Consequently the height of a 50-year wave as estimated by this method is likely to be greater than that estimated from the method of using a long-term distribution of Hs.

III.3 References

BATTJES J A 1970. Long-term wave height distribution at seven stations around the British Isles. National Institute of Oceanography, Internal Report No A44.

FISHER R A AND TIPPETT L H C 1928. Limiting forms of the frequency distribution of the largest or smallest member of a sample. Proceedings of the Cambridge Philosophical Society 24, 180-190.

GUMBEL E J 1958. Statistics of Extremes. New York: Columbia University Press. 371 pp.

TANN H M 1976. The estimation of wave parameters for the design of offshore structures. Institute of Oceanographic Sciences, Report No 23.

APPENDIX IV

Kinnairds Head Waverider deployment history.

YEAR	DATE	EVENT
1979	19 October	Buoy deployed.
	25 October	Receiving system commissioned.
	21 November	Buoy lost from station (unknown to IOS).
1980	04 January	Buoy found drifting, instruction to replace issued.
	16 January	Buoy deployed, transmission frquency in 29MHZ band.
	28 January	Buoy found drifting off Scrabster (NE Scotland), instruction to replace issued.
	23 February	Buoy deployed.
	25 February	Alarm light system installed, Microdata logger replaced.
	25 May	Buoy adrift, instruction to replace issued.
	09 June	Buoy deployed.
	18/19 June	Aerial system changed.
	25 June	Requested replacement of buoy transmitter.
	01 July	Buoy adrift, instruction to replace issued.
	25 July	Buoy deployed.
	08 September	No signal at shore station, instruction to replace issued.
	04 October	Buoy deployed. Telemetry problems, long periods of nil data.
	27 November	No signal at shore station, instruction to replace issued.
	13 December	Buoy (higher output O/P) deployed.

	18 December	No signals at shore station, instruction to replace issued.
1981	08 January	Buoy deployed.
	05 May	Buoy exchanged.
	29 May	Poor signal, instruction to replace issued.
	04 June	Buoy deployed.
	10 June	No signal at shore station.
	25 June	Instruction to replace issued.
	08 July	Buoy deployed.
1982	26 January	No signal at shore station.
	28 February	End of contract.

MERCATOR PROJECTION

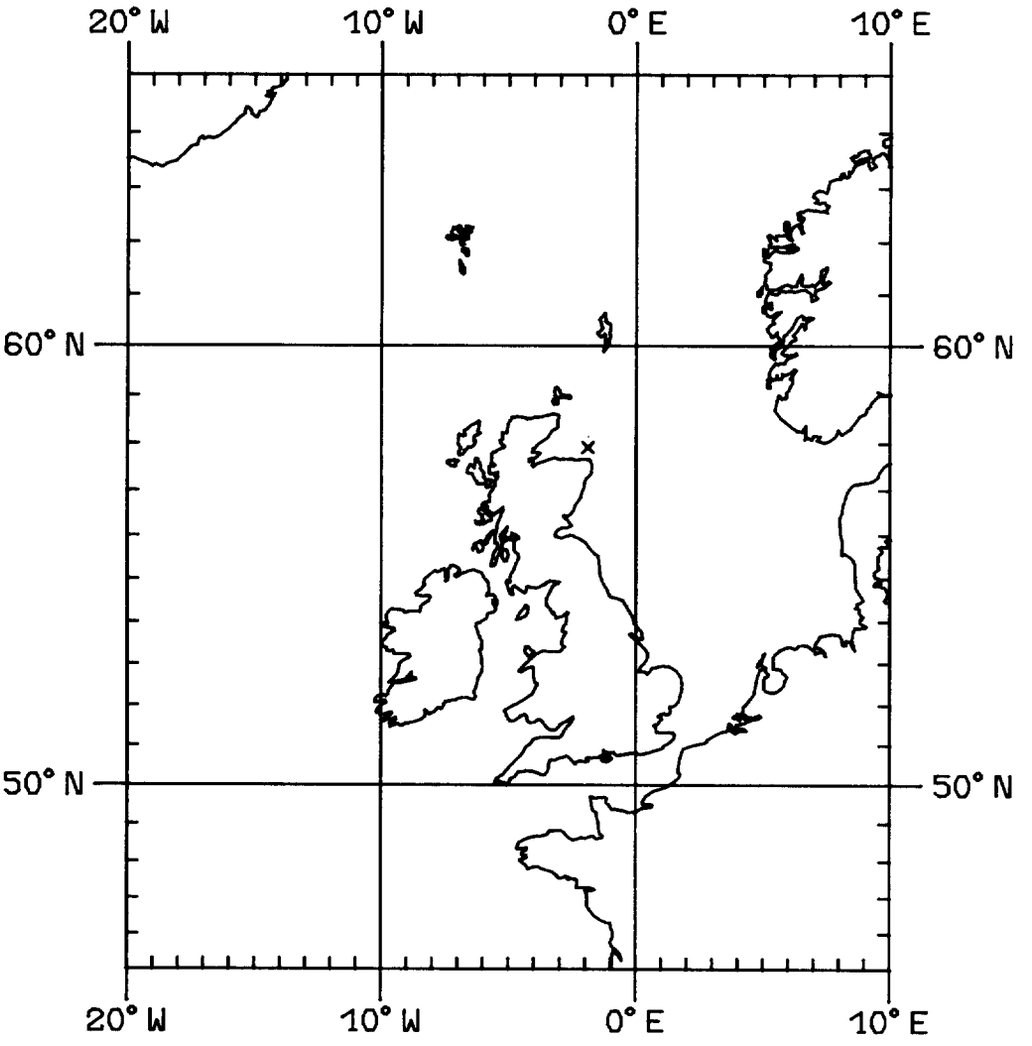

KINNAIRDS HEAD, NORTH SEA

POSITION 57 55 N 001 54 W

FIGURE 1.1

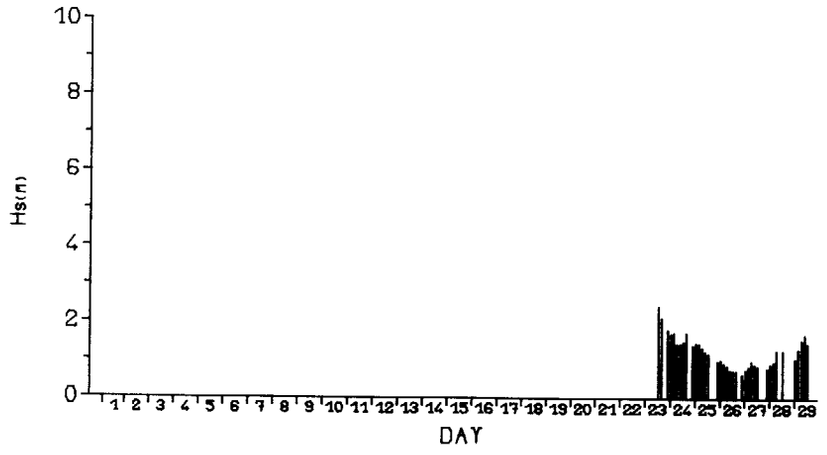

FEB 1980

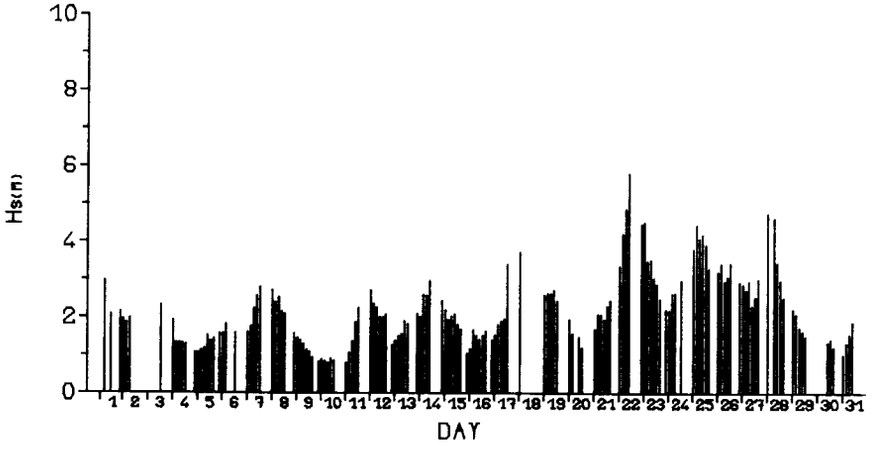

MAR 1980

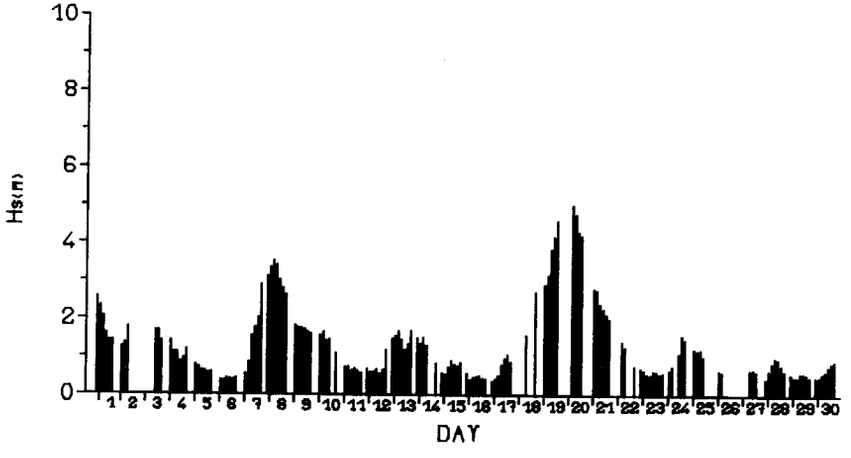

APR 1980

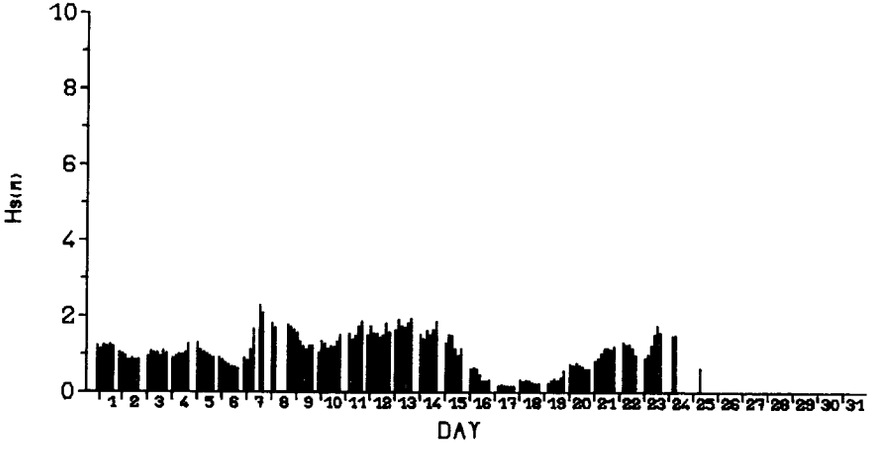

MAY 1980

TIME SERIES OF Hs

KINNAIRDS HEAD FEB 1980 - JAN 1982

FIG 1.4(A)

KH8082

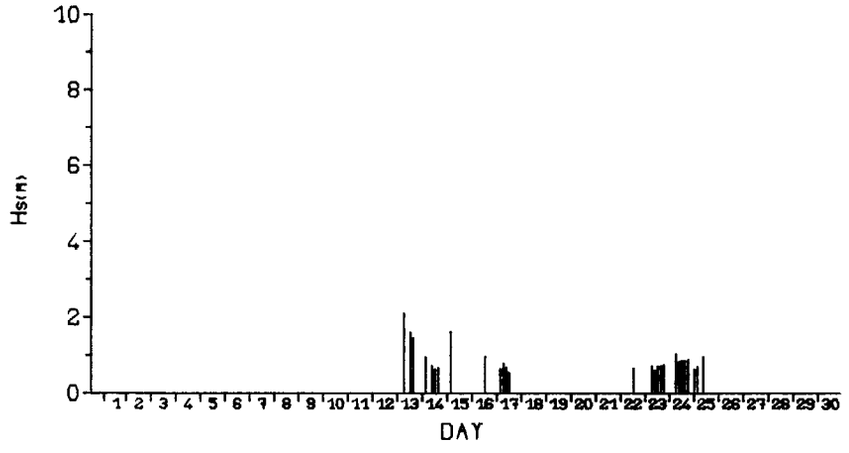

JUN 1980

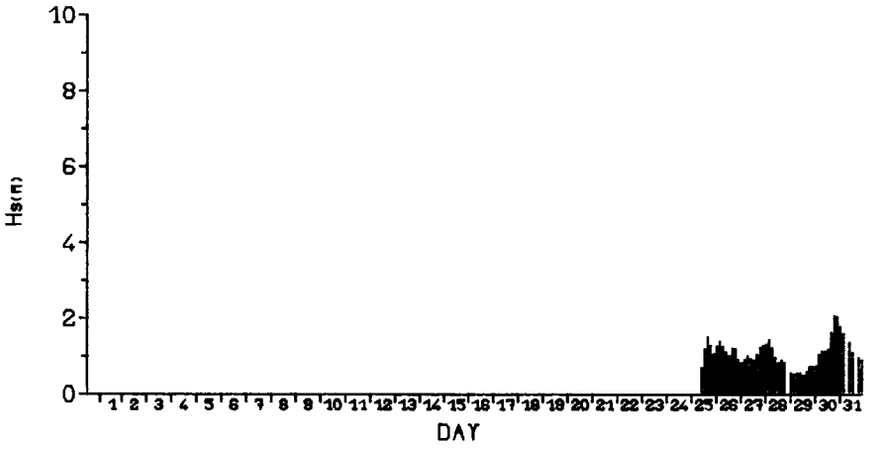

JUL 1980

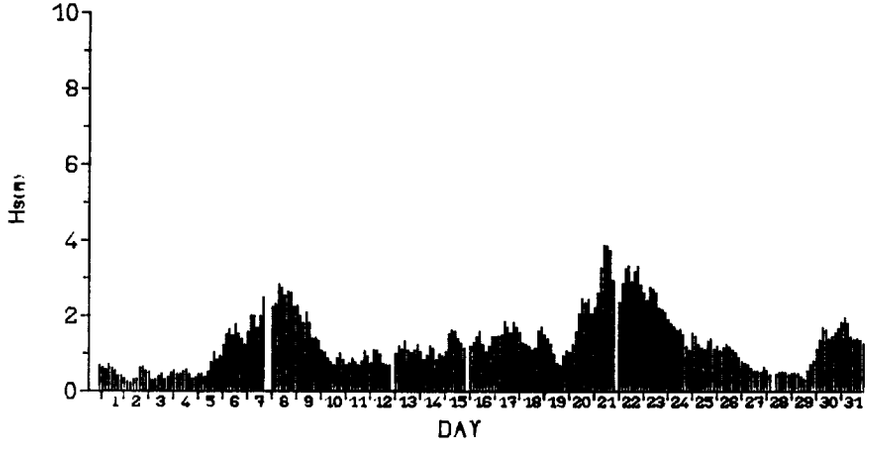

AUG 1980

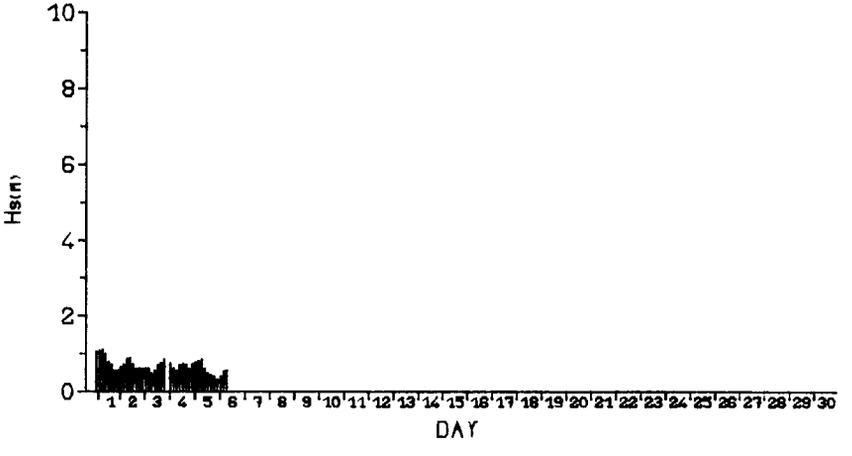

SEP 1980

TIME SERIES OF Hs

KINNAIRDS HEAD FEB 1980 - JAN 1982

FIG 1.4(B)

KH8082

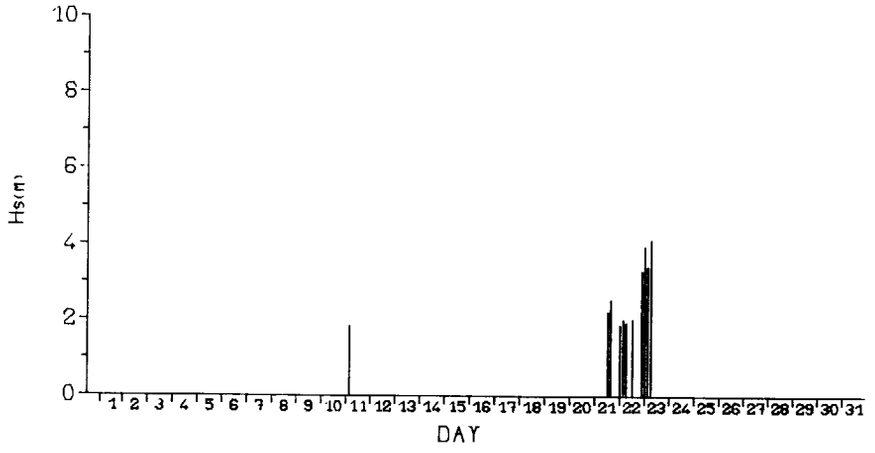

OCT 1980

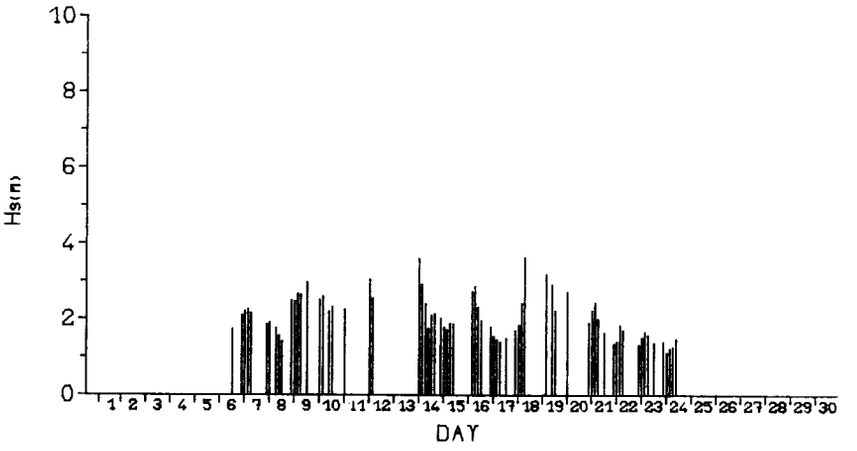

NOV 1980

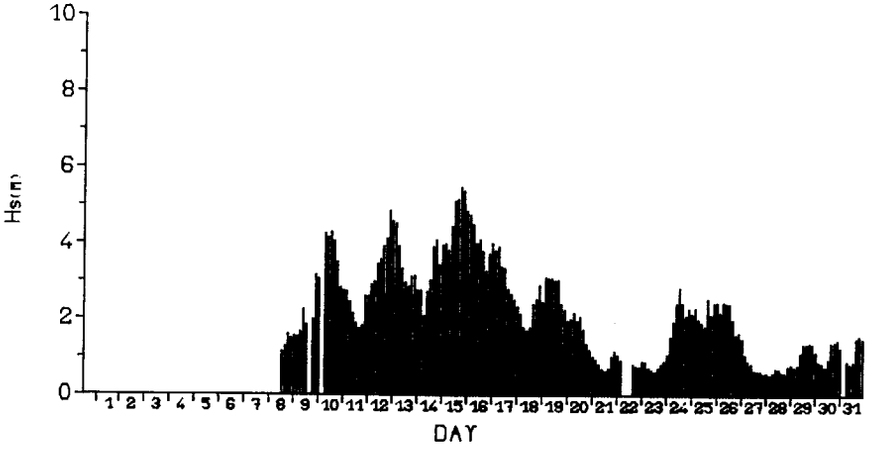

JAN 1981

TIME SERIES OF Hs

KINNAIRDS HEAD FEB 1980 - JAN 1982

FIG 1.4(C)

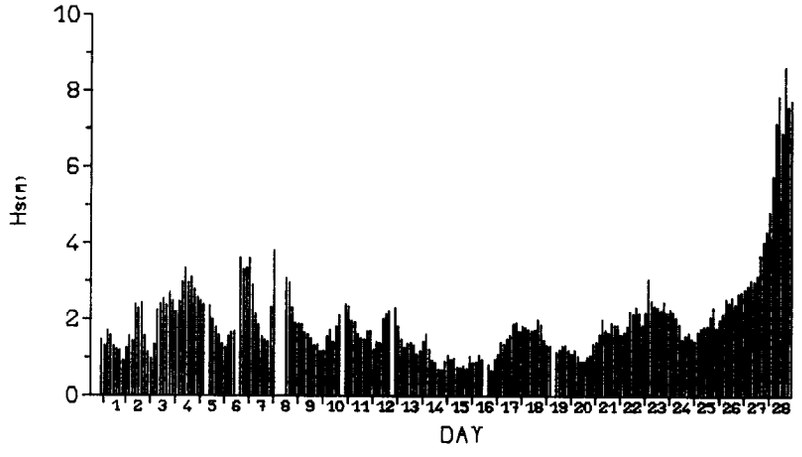

FEB 1981

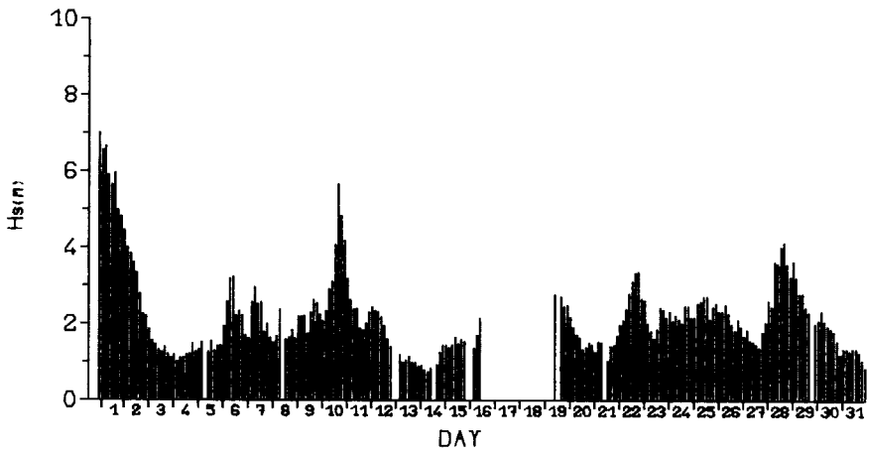

MAR 1981

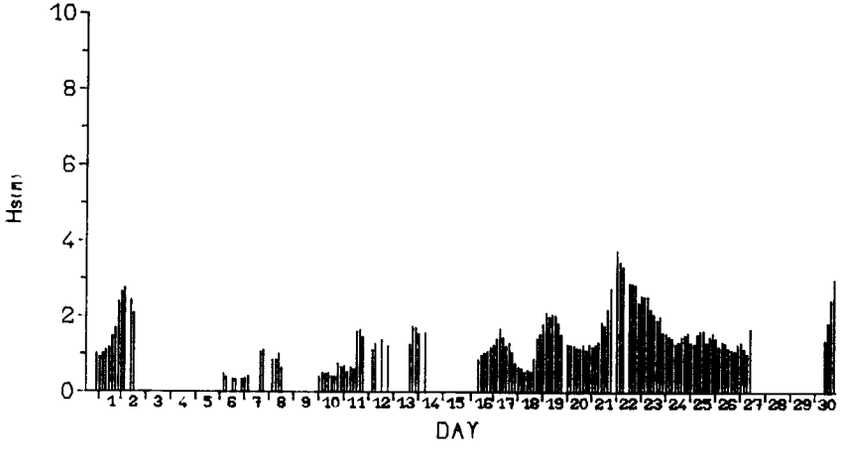

APR 1981

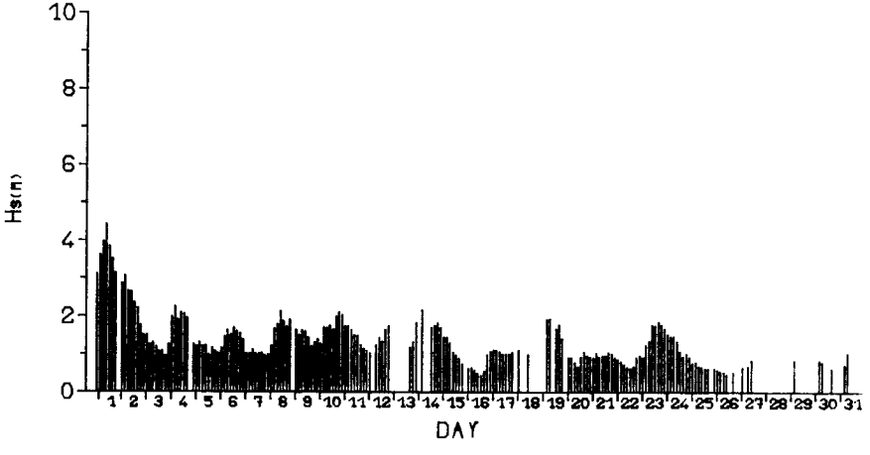

MAY 1981

TIME SERIES OF Hs

KINNAIRDS HEAD FEB 1980 - JAN 1982

FIG 1.4(D)

K48082

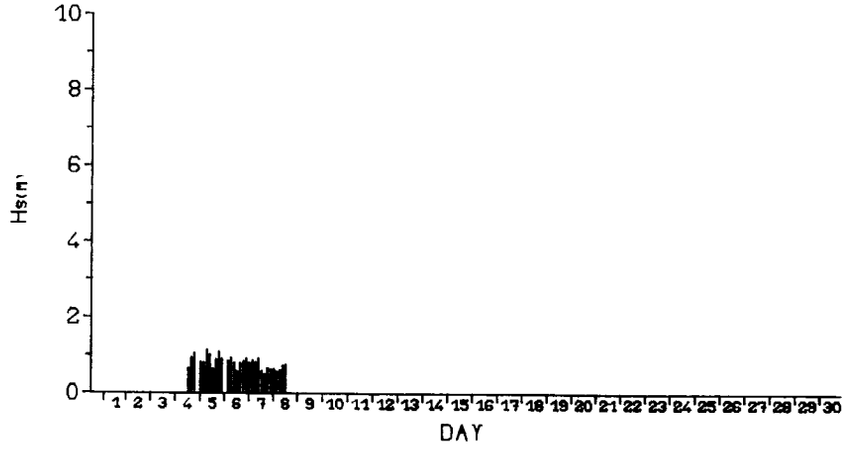

JUN 1981

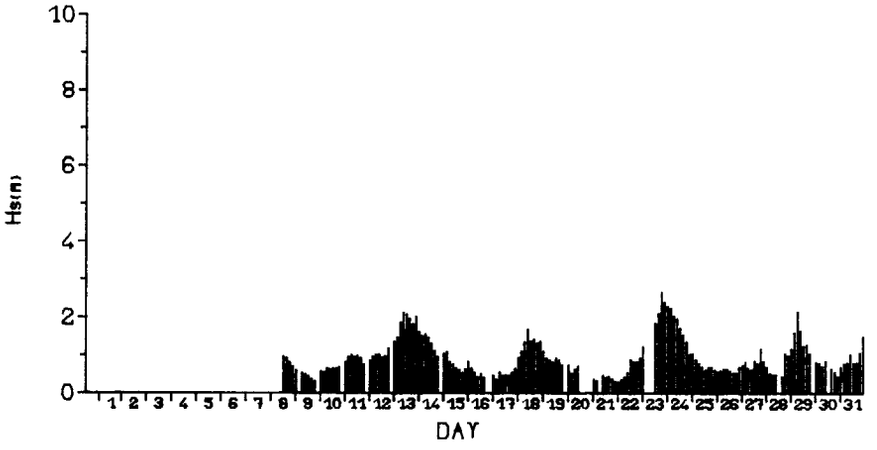

JUL 1981

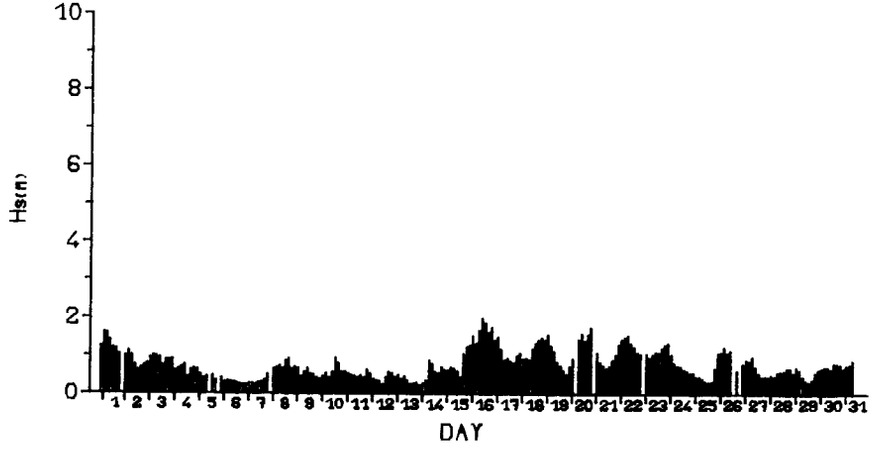

AUG 1981

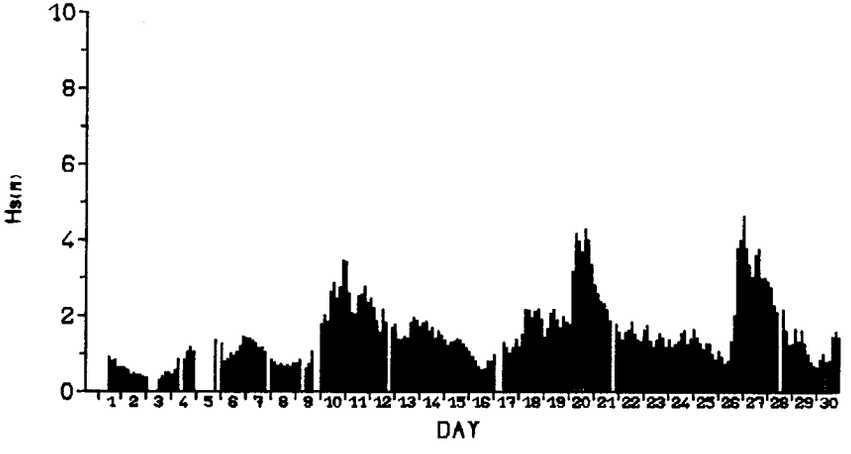

SEP 1981

TIME SERIES OF Hs

KINNAIRDS HEAD FEB 1980 - JAN 1982

FIG 1.4(E)

KH8082

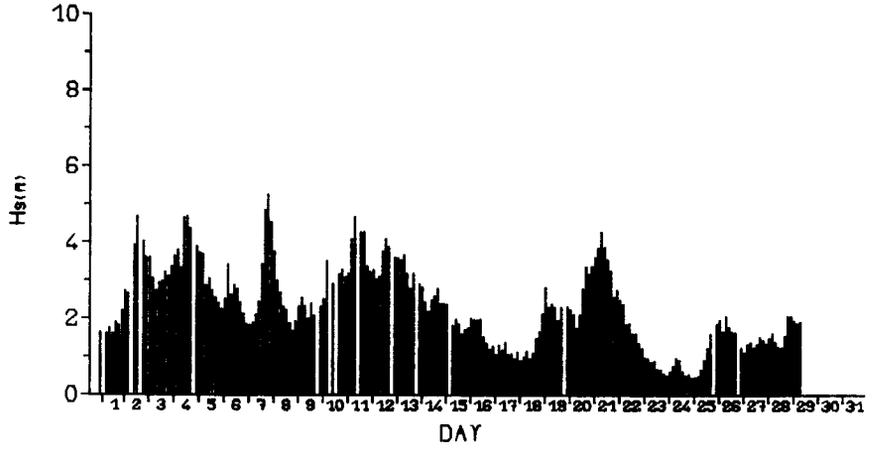

OCT 1981

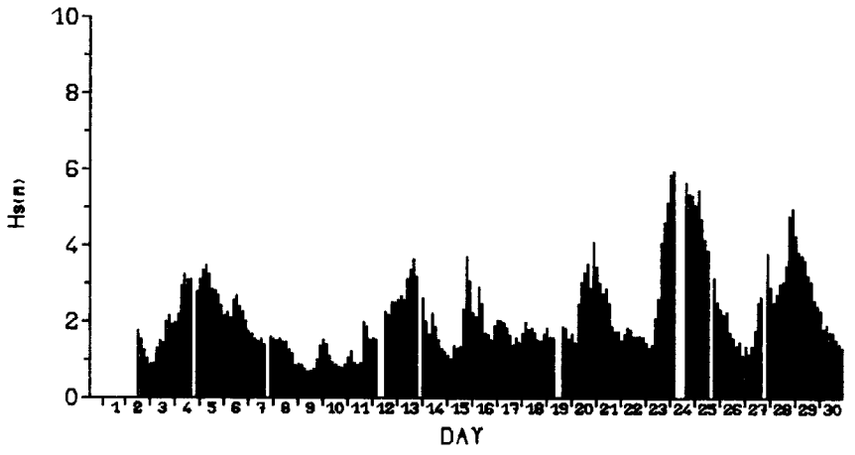

NOV 1981

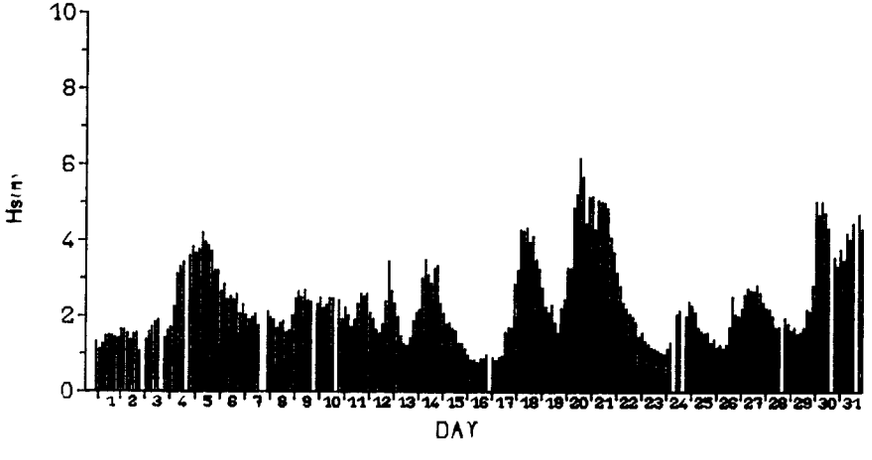

DEC 1981

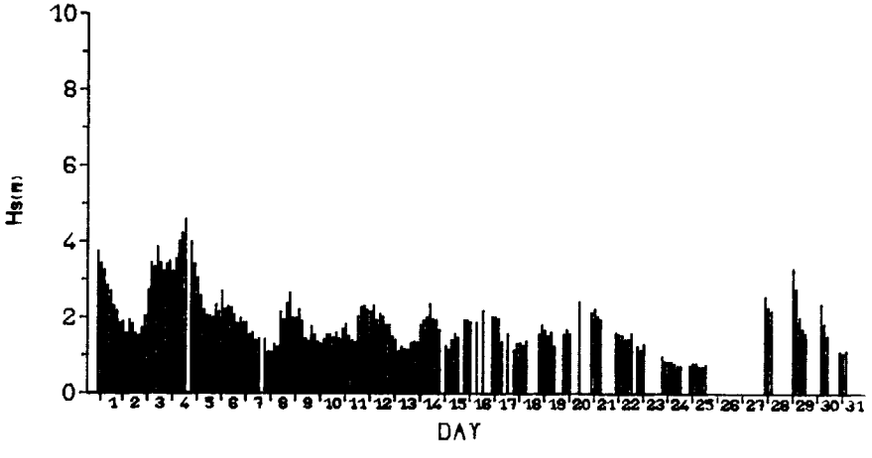

JAN 1982

TIME SERIES OF Hs

KINNAIRDS HEAD FEB 1980 - JAN 1982

FIG 1.4(F)

KH8082

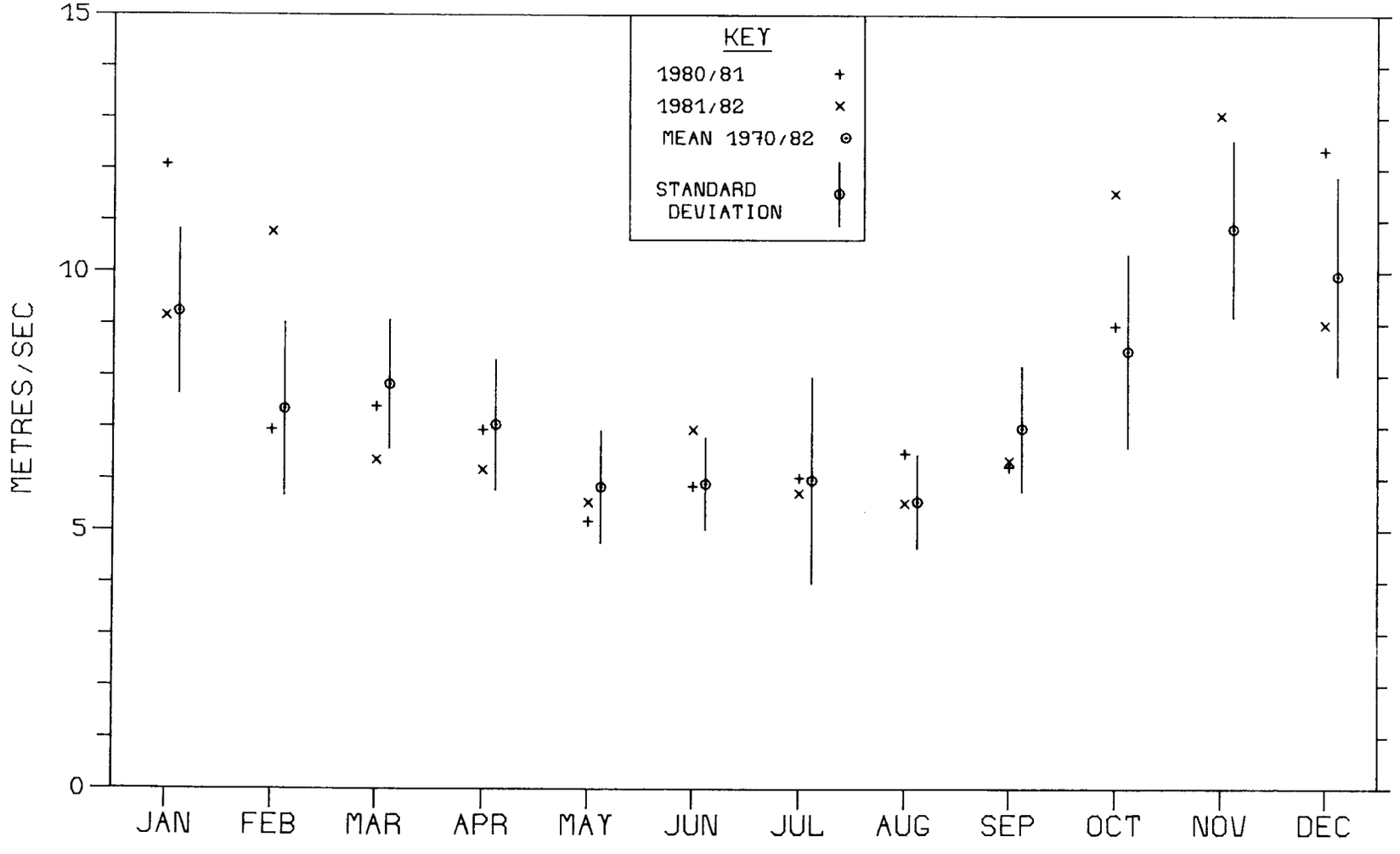

MEAN AND STANDARD DEVIATION OF THE MONTHLY MEAN OF WIND SPEED

FRASERBURGH FEB 1970 - JAN 1982

FIG 2.1

KH8082

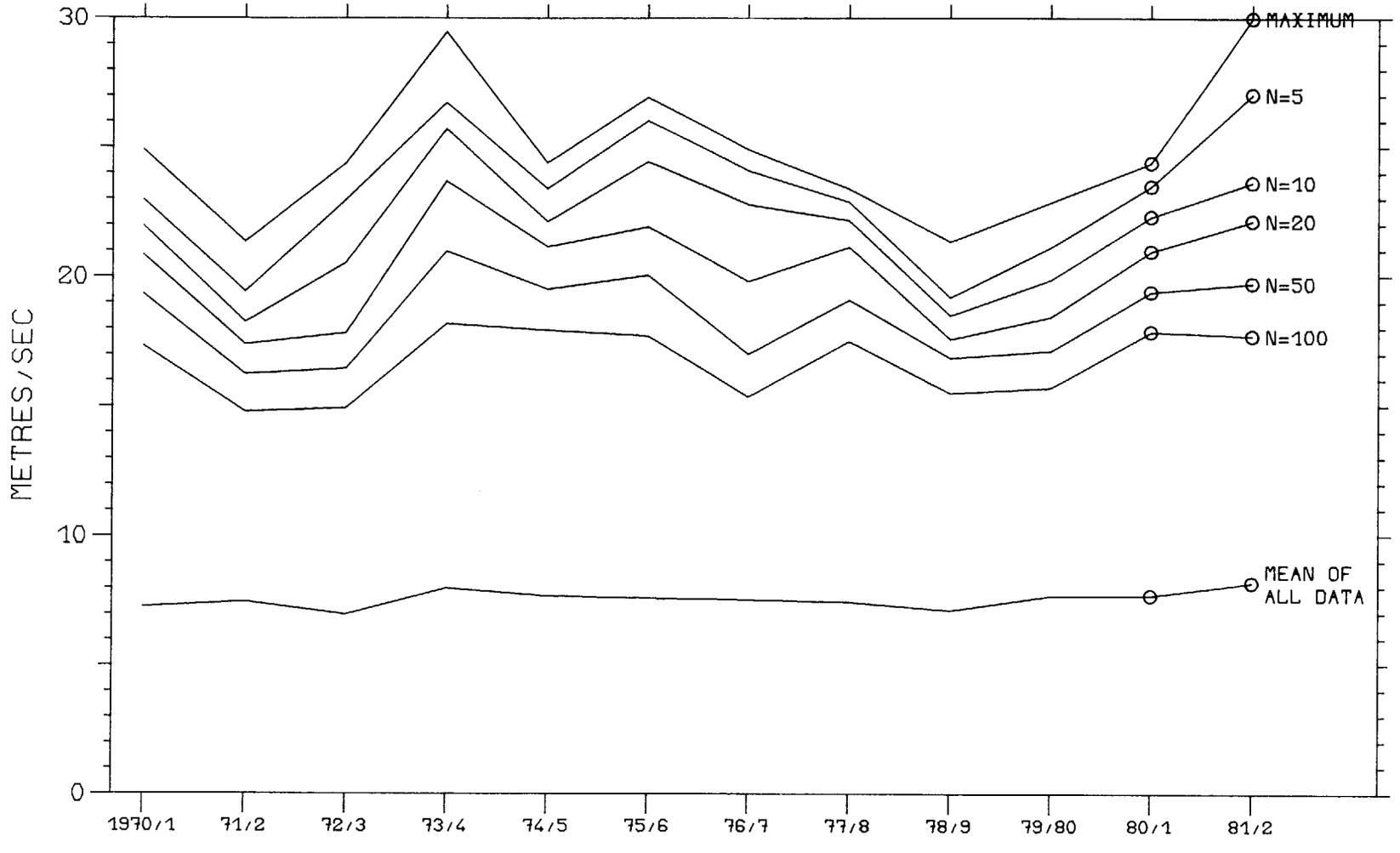

MEAN OF N LARGEST VALUES OF WIND SPEED

FRASERBURGH FEB 1970 - JAN 1982

FIG 2.2

KH8082

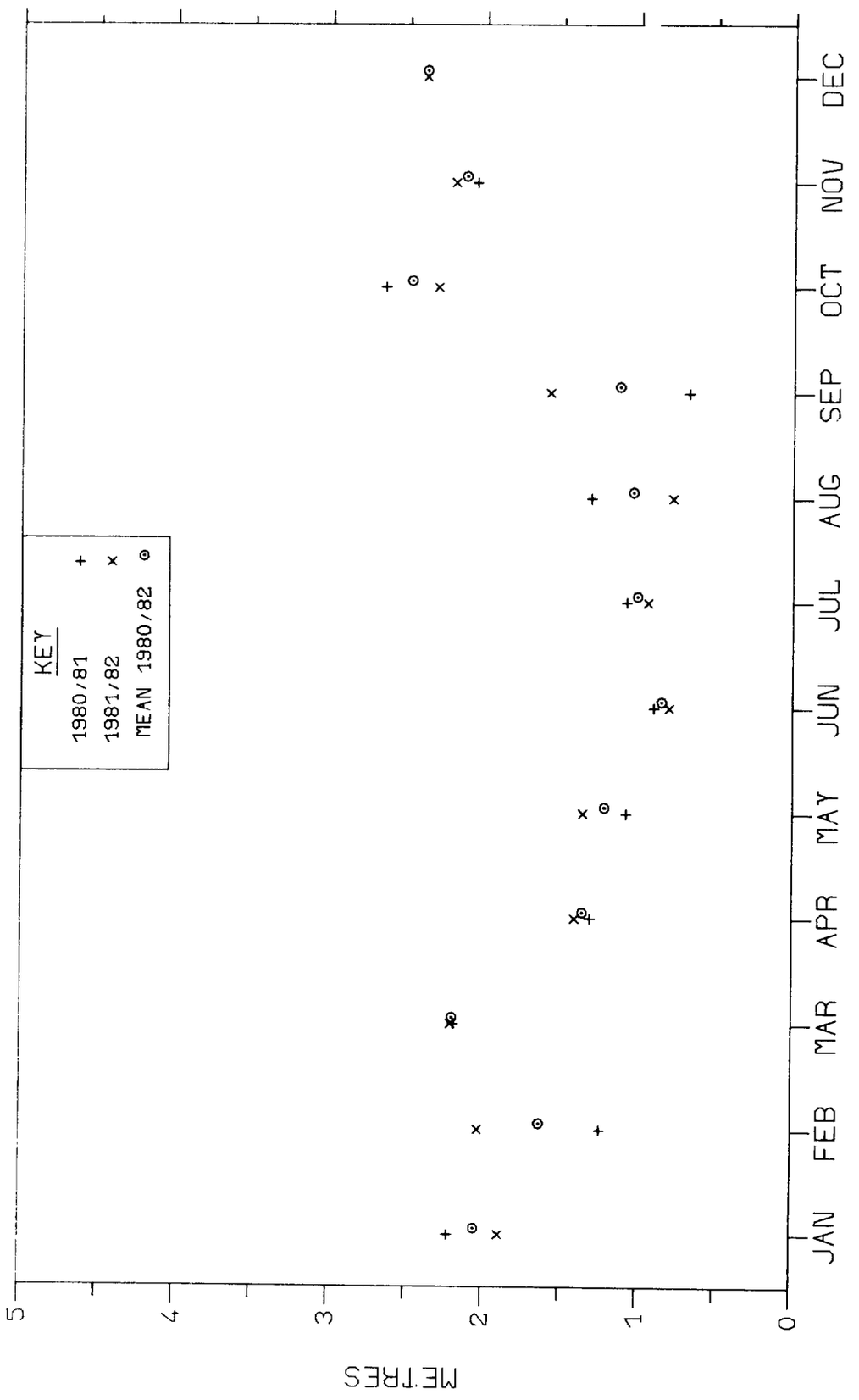

MONTHLY MEANS OF Hs FOR EACH YEAR

KINNAIRDS HEAD FEB 1980 - JAN 1982

FIG 3.1.1

KH80082

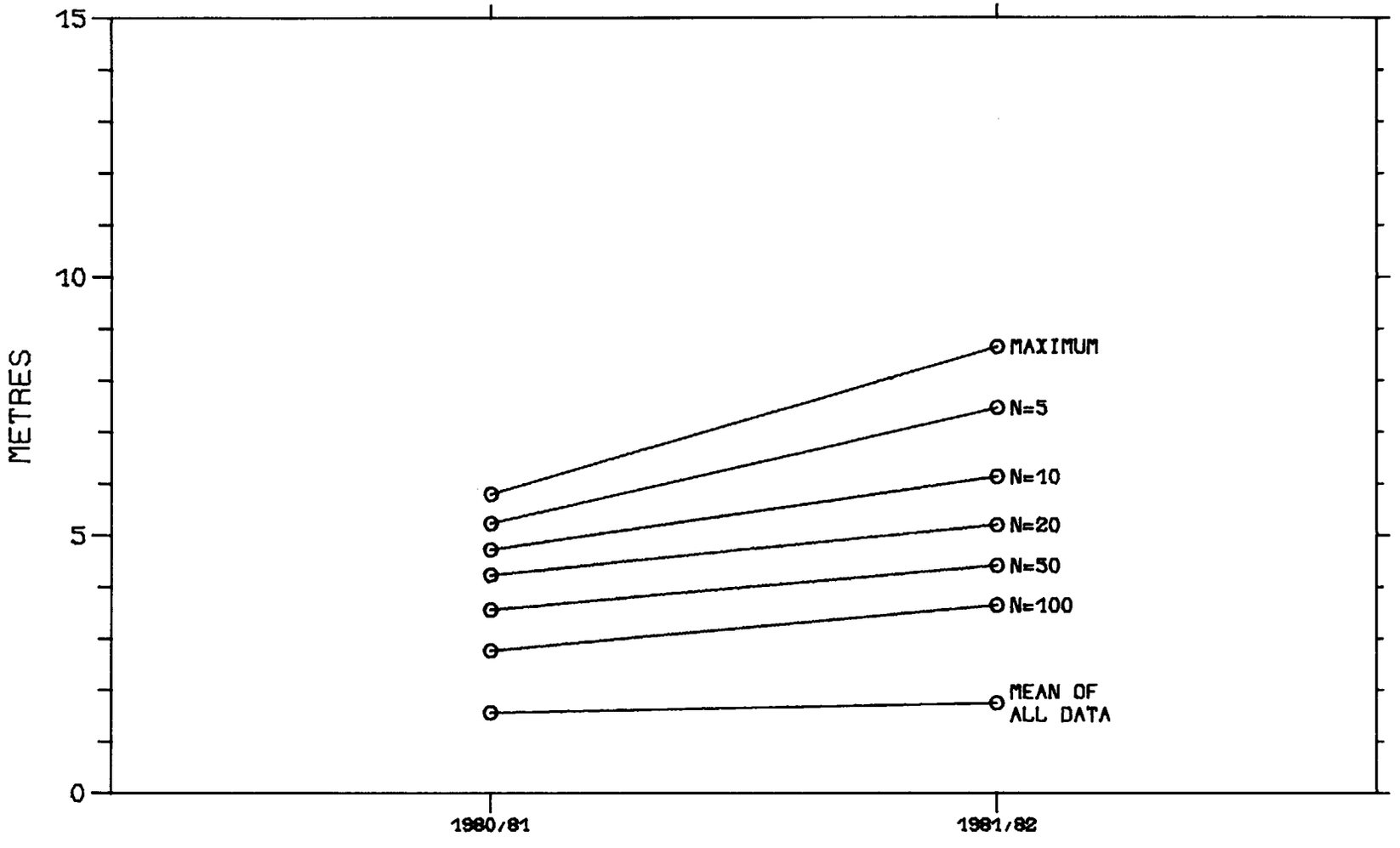

MEAN OF N LARGEST VALUES OF Hs

KINNAIRDS HEAD FEB 1980 - JAN 1982

FIG 3.1.2

KH8082

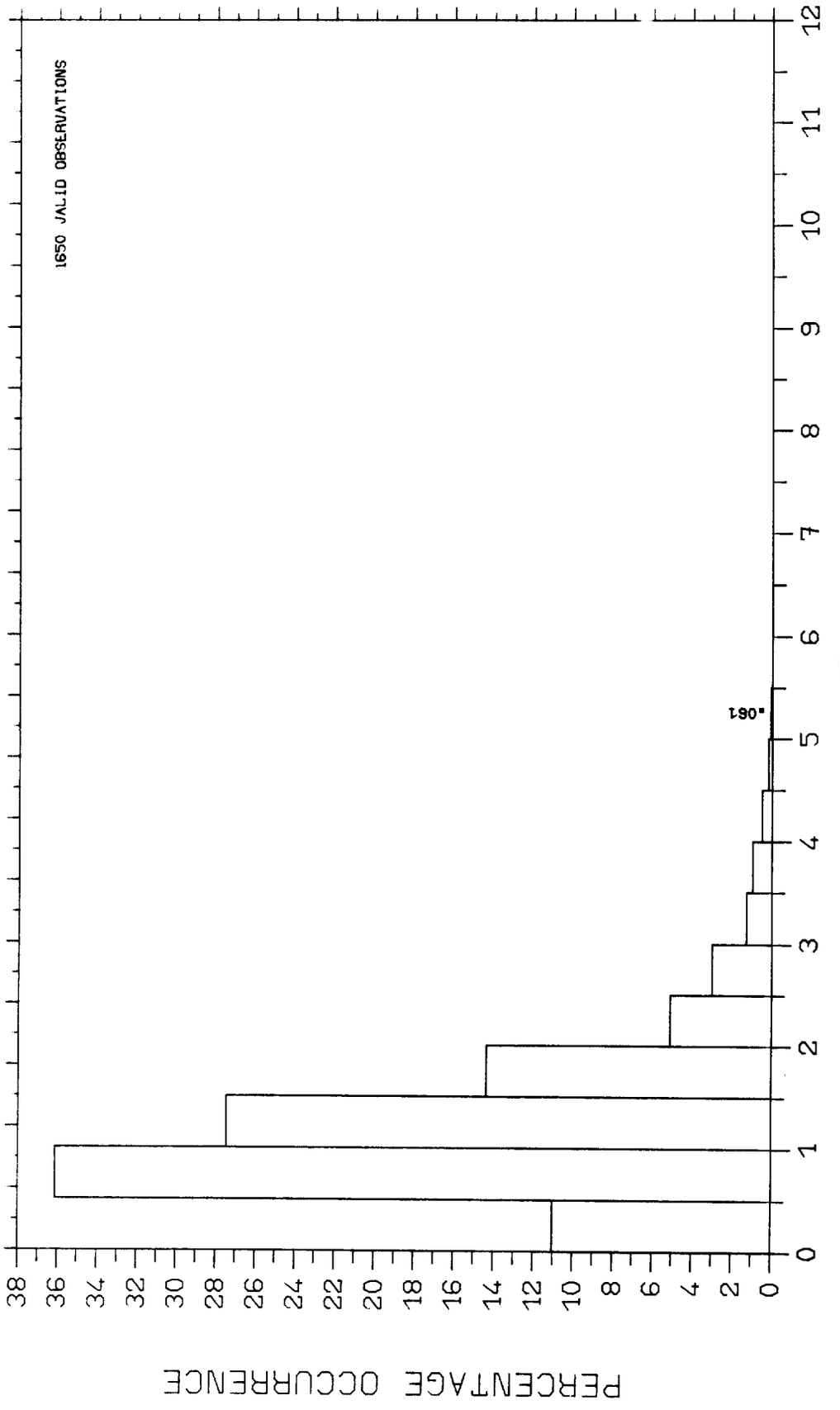

PERCENTAGE OCCURRENCE HISTOGRAM

KINNAIRDS HEAD FEB 1980 - JAN 1982 SUMMERS

FIG 3.2.1.1

KH8082

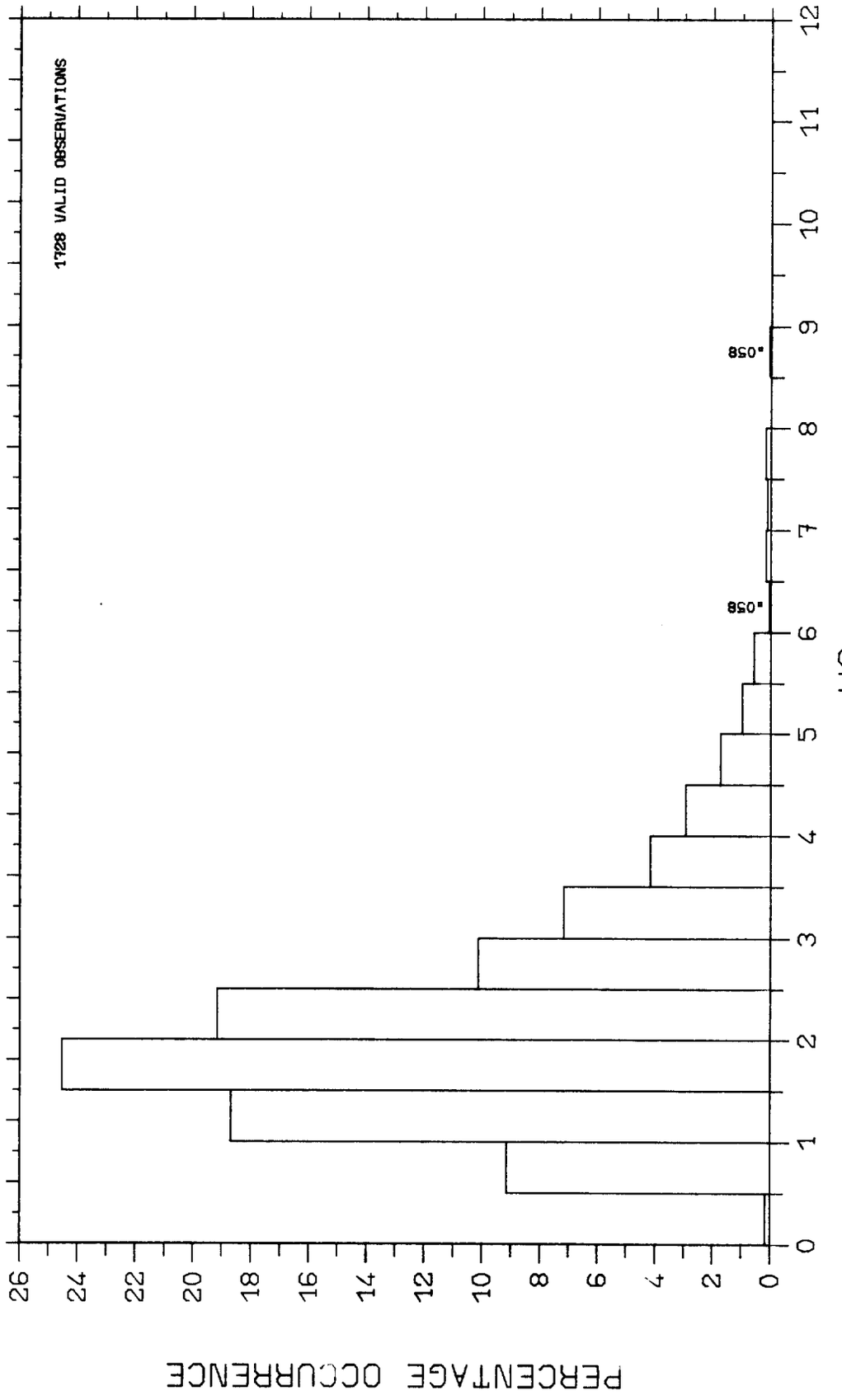

PERCENTAGE OCCURRENCE HISTOGRAM

KINNAIRDS HEAD FEB 1980 - JAN 1982 WINTERS

FIG 3.2.1.2

KH8082

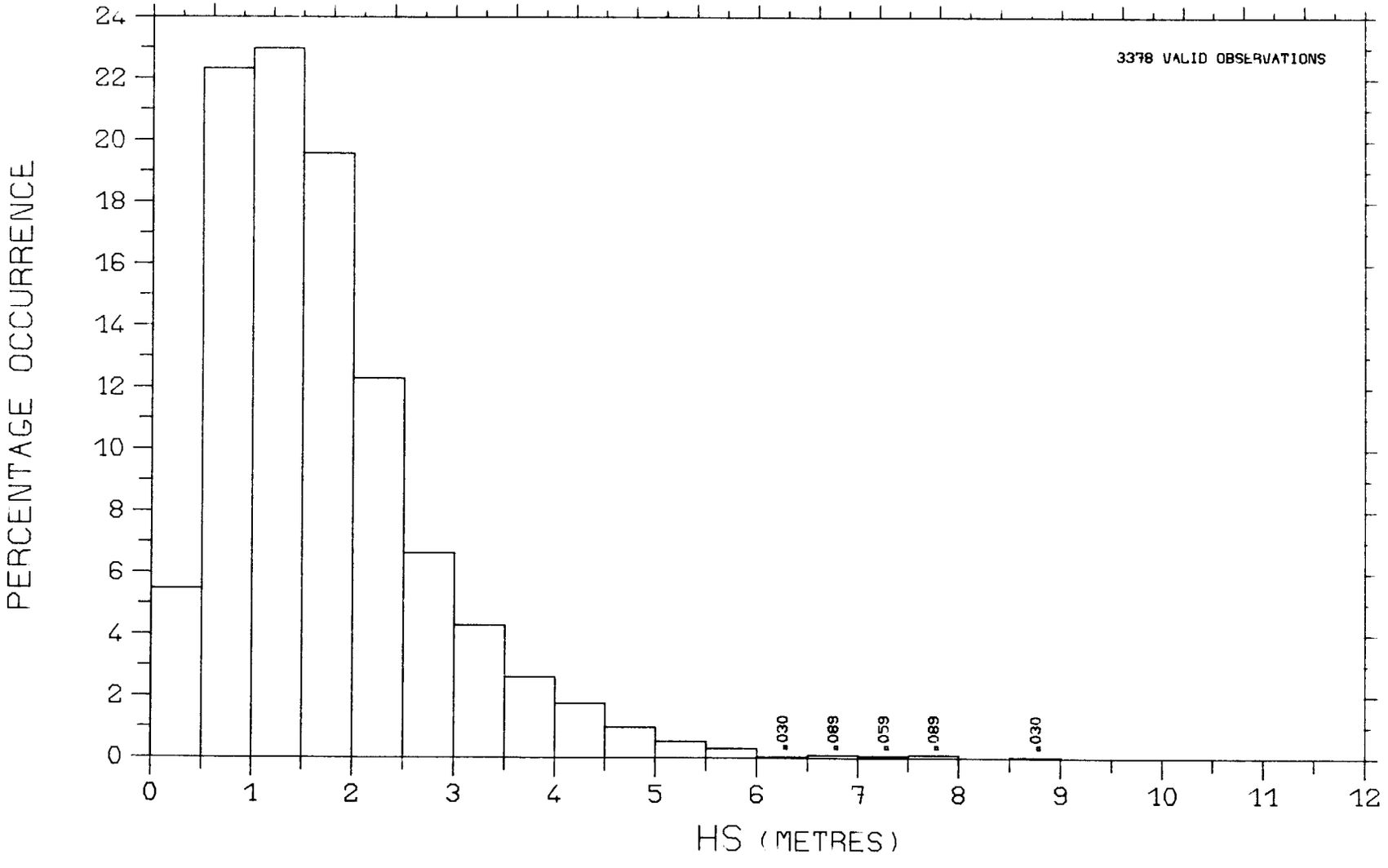

PERCENTAGE OCCURRENCE HISTOGRAM

KINNAIRDS HEAD FEB 1980 - JAN 1982

FIG 3.2.1.3

KH8082

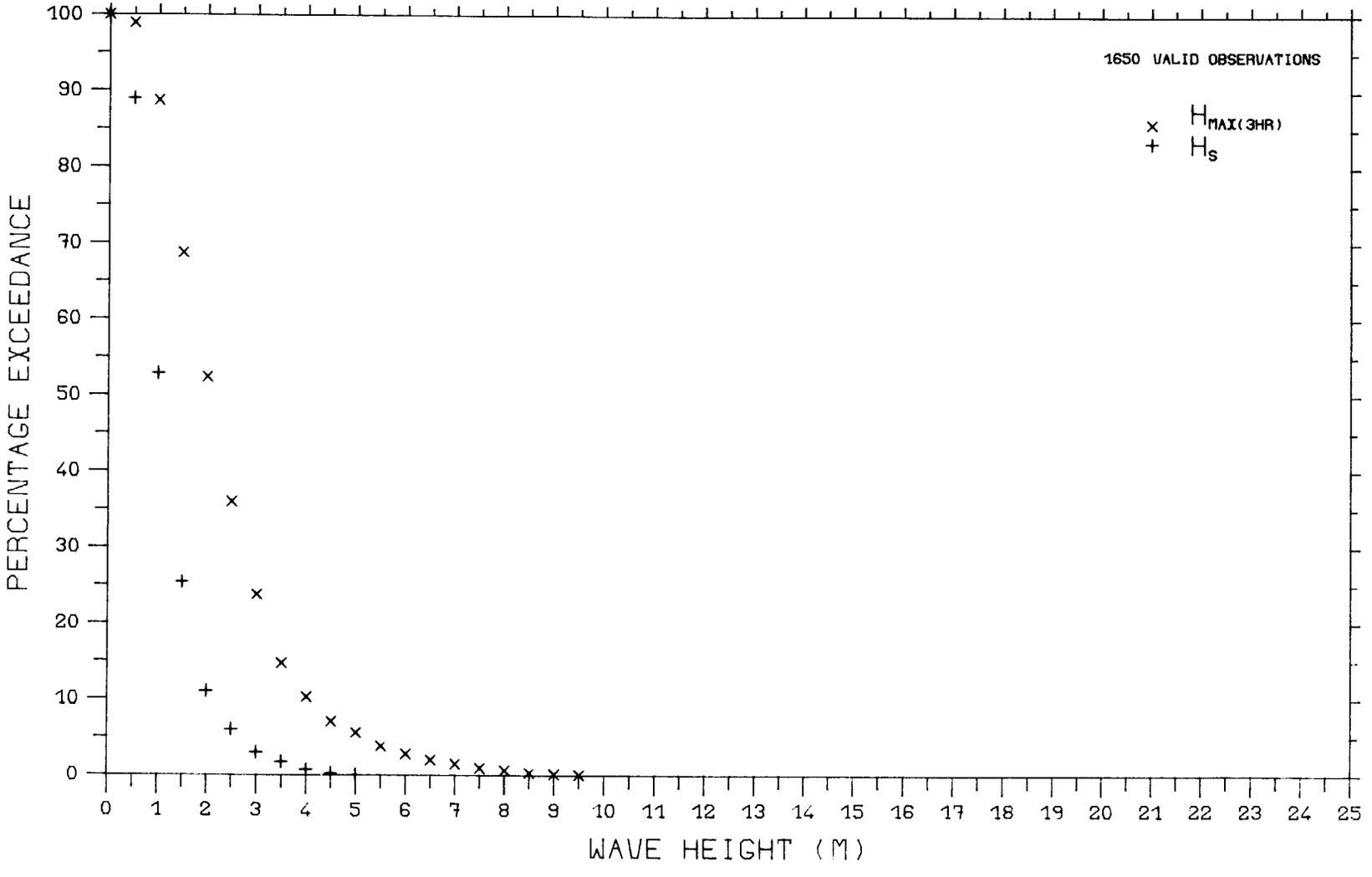

PERCENTAGE EXCEEDANCE OF H_S AND $H_{MAX(3HR)}$

KINNAIRDS HEAD JAN 1980 - FEB 1982 SUMMERS

FIG 3.2.2.1

KH6082

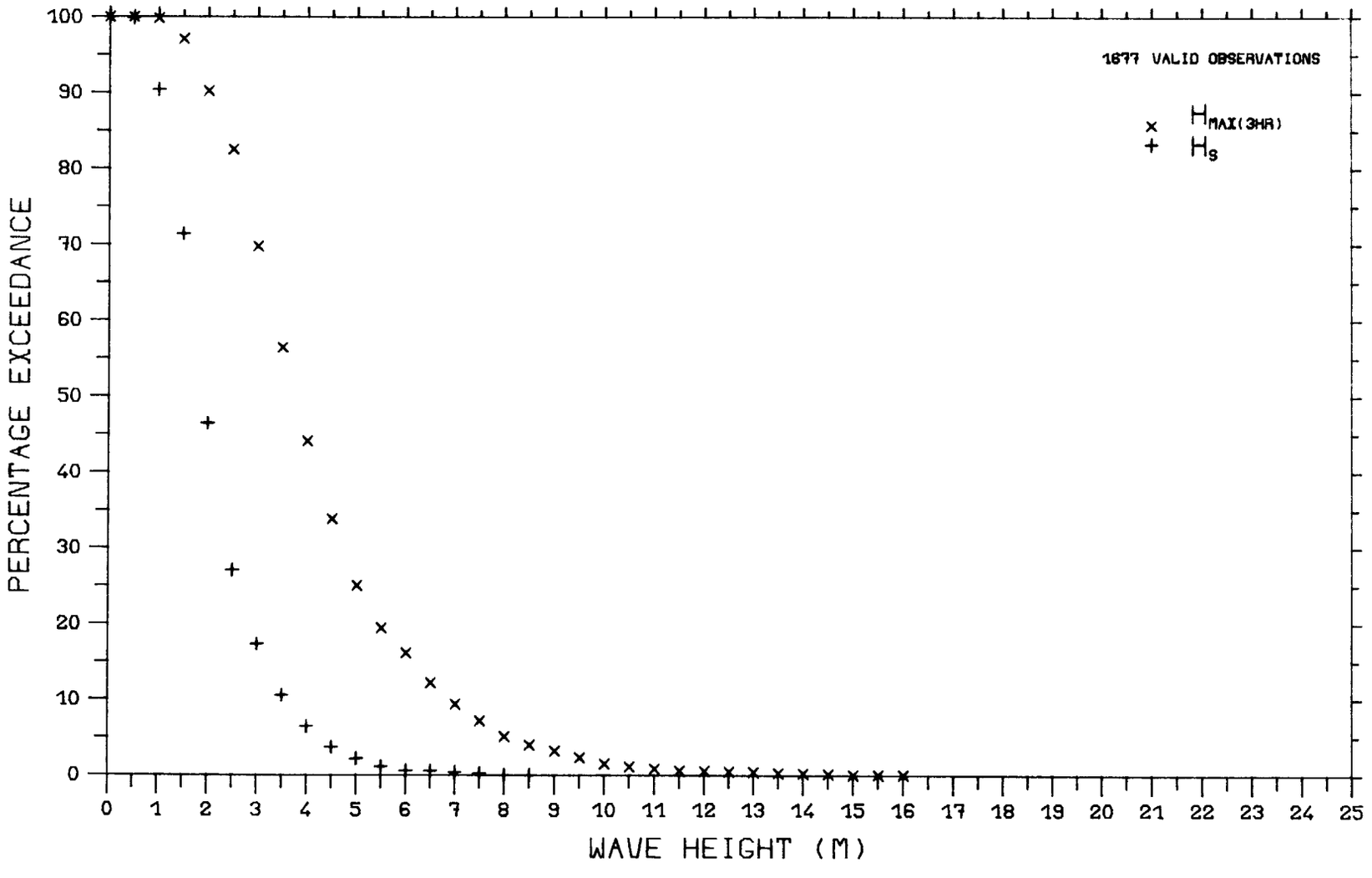

PERCENTAGE EXCEEDANCE OF H_S AND $H_{MAX(3HR)}$

KINNAIRDS HEAD JAN 1980 - FEB 1982 WINTERS

FIG 3.2.2.2

KH8082

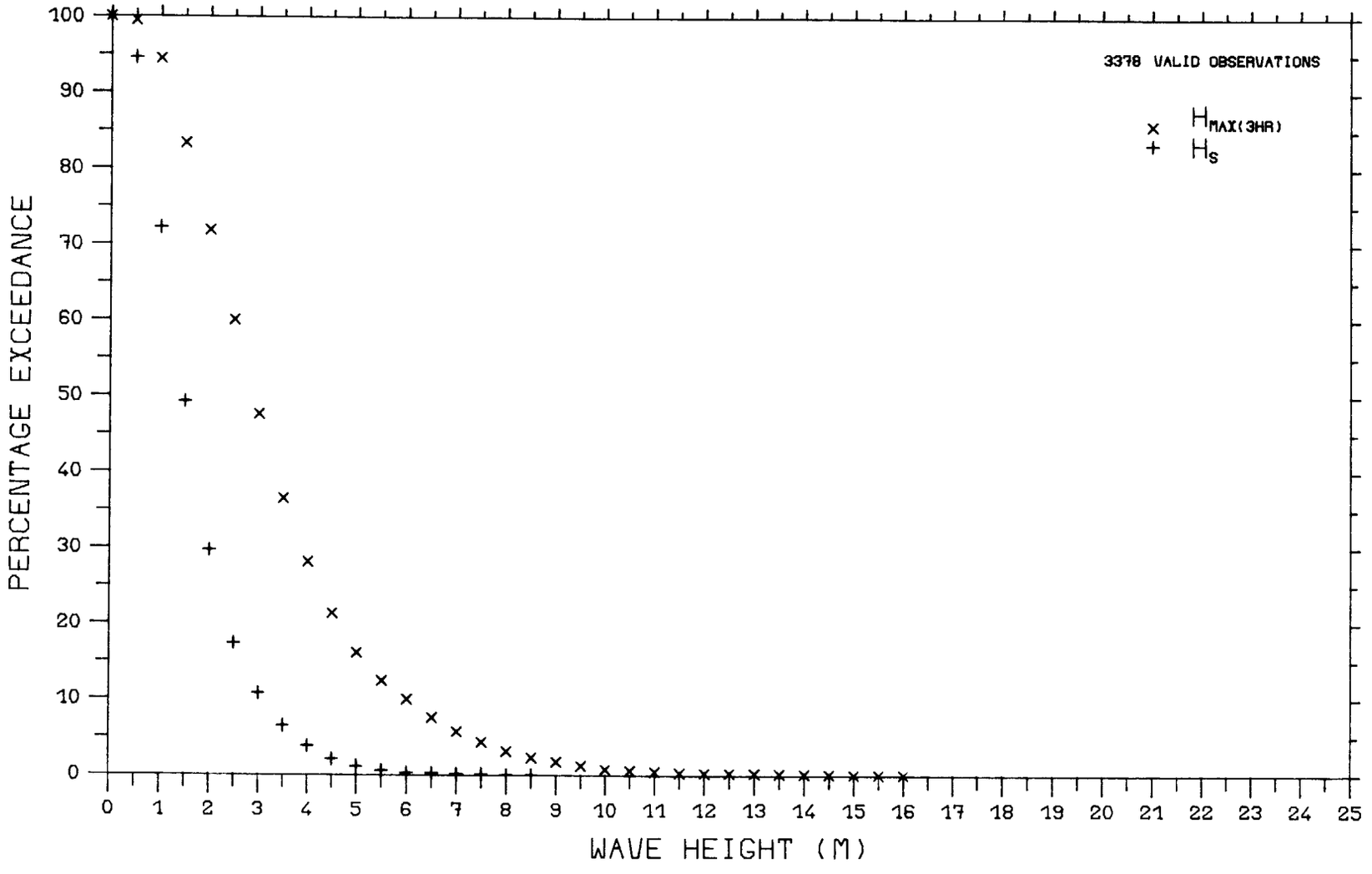

PERCENTAGE EXCEEDANCE OF H_S AND $H_{MAX(3HR)}$

KINNAIRDS HEAD JAN 1980 - FEB 1982

FIG 3.2.2.3

KH8082

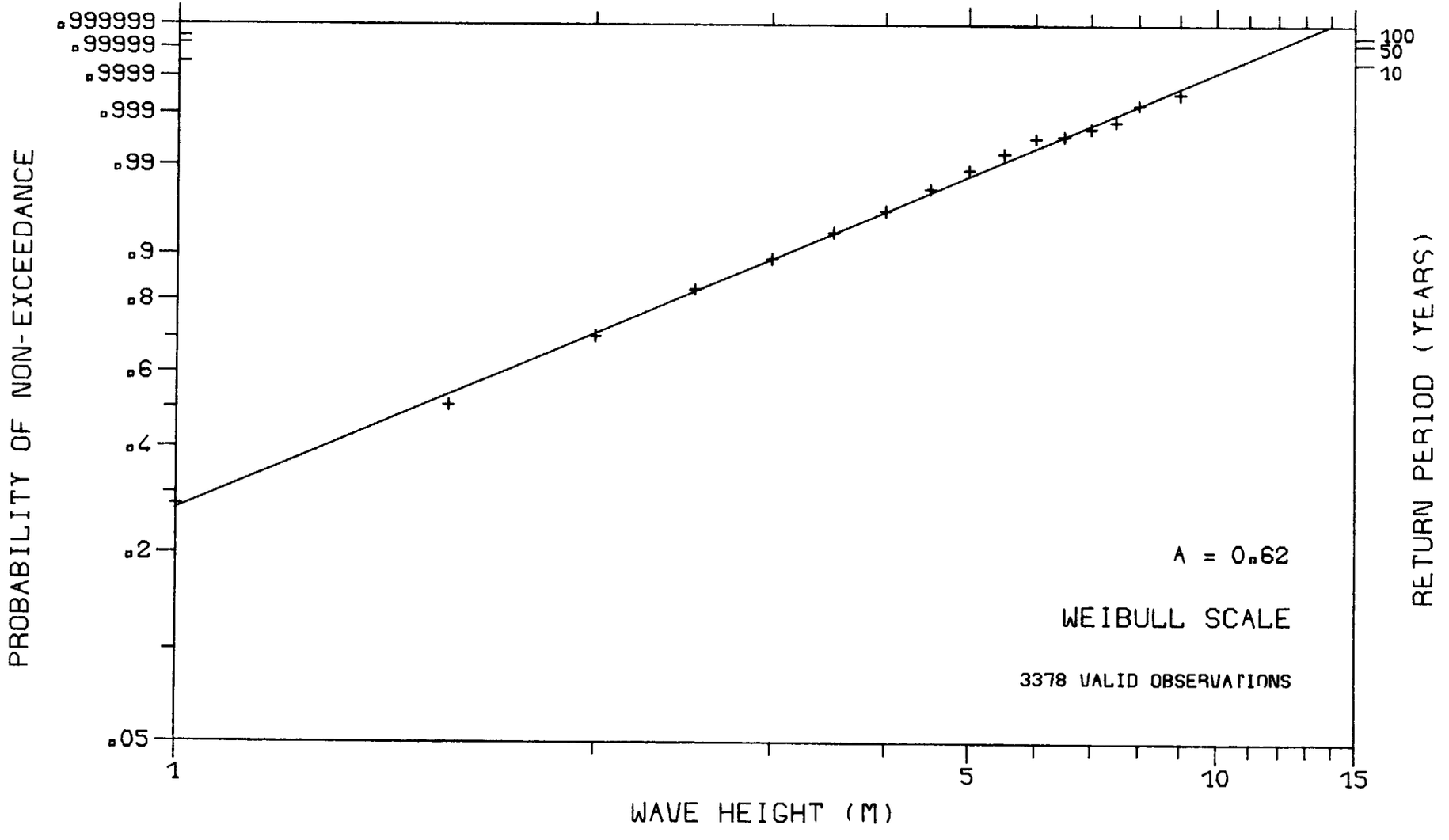

CUMULATIVE DISTRIBUTION OF WAVE HEIGHT, HS

KINNAIRDS HEAD FEB 1980 - JAN 1982

FIG 3.3.1

KH8082

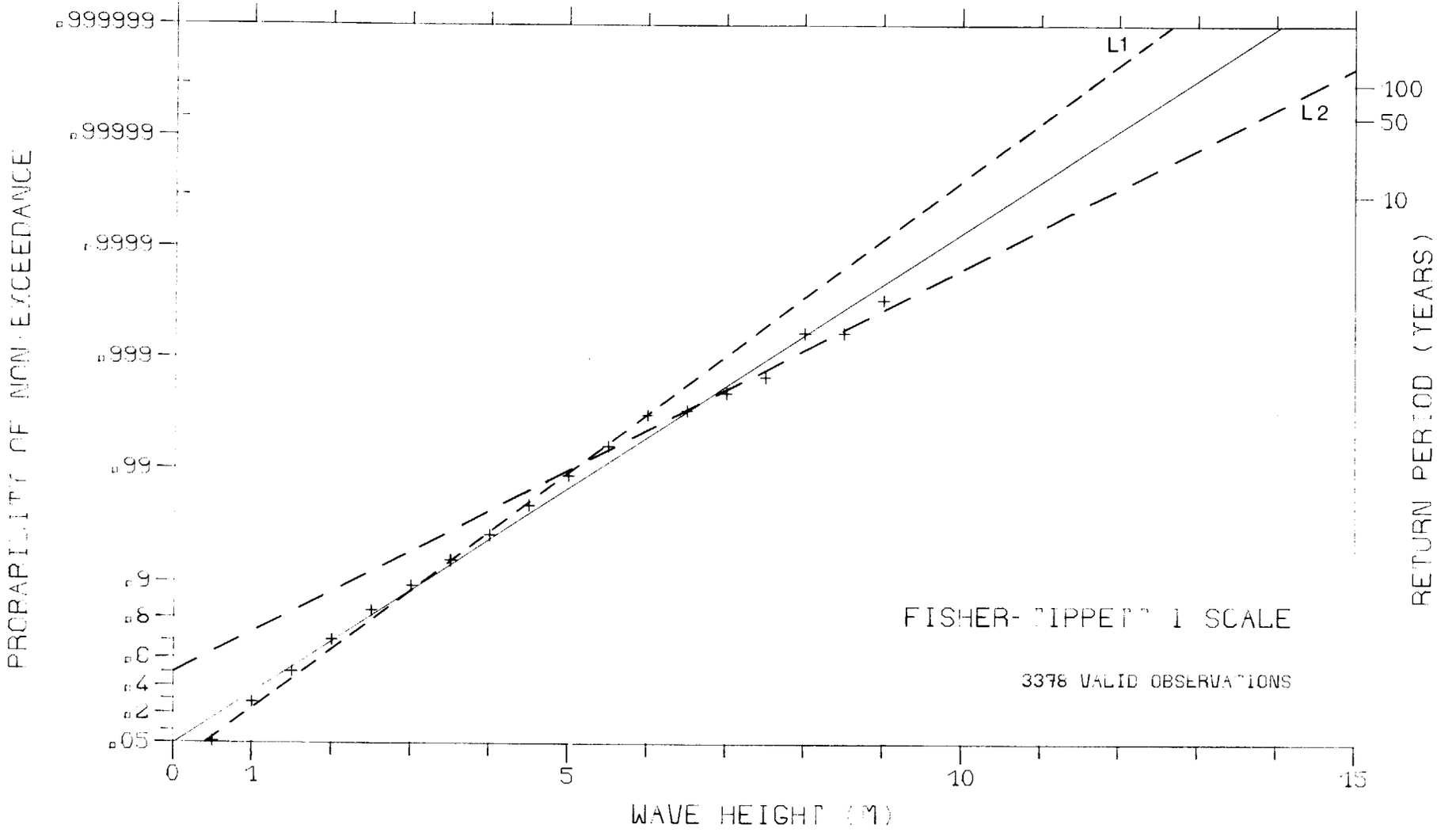

CUMULATIVE DISTRIBUTION OF WAVE HEIGHT, HS

KINNAIRDS HEAD FEB 1980 - JAN 1982

FIG 3.3.2

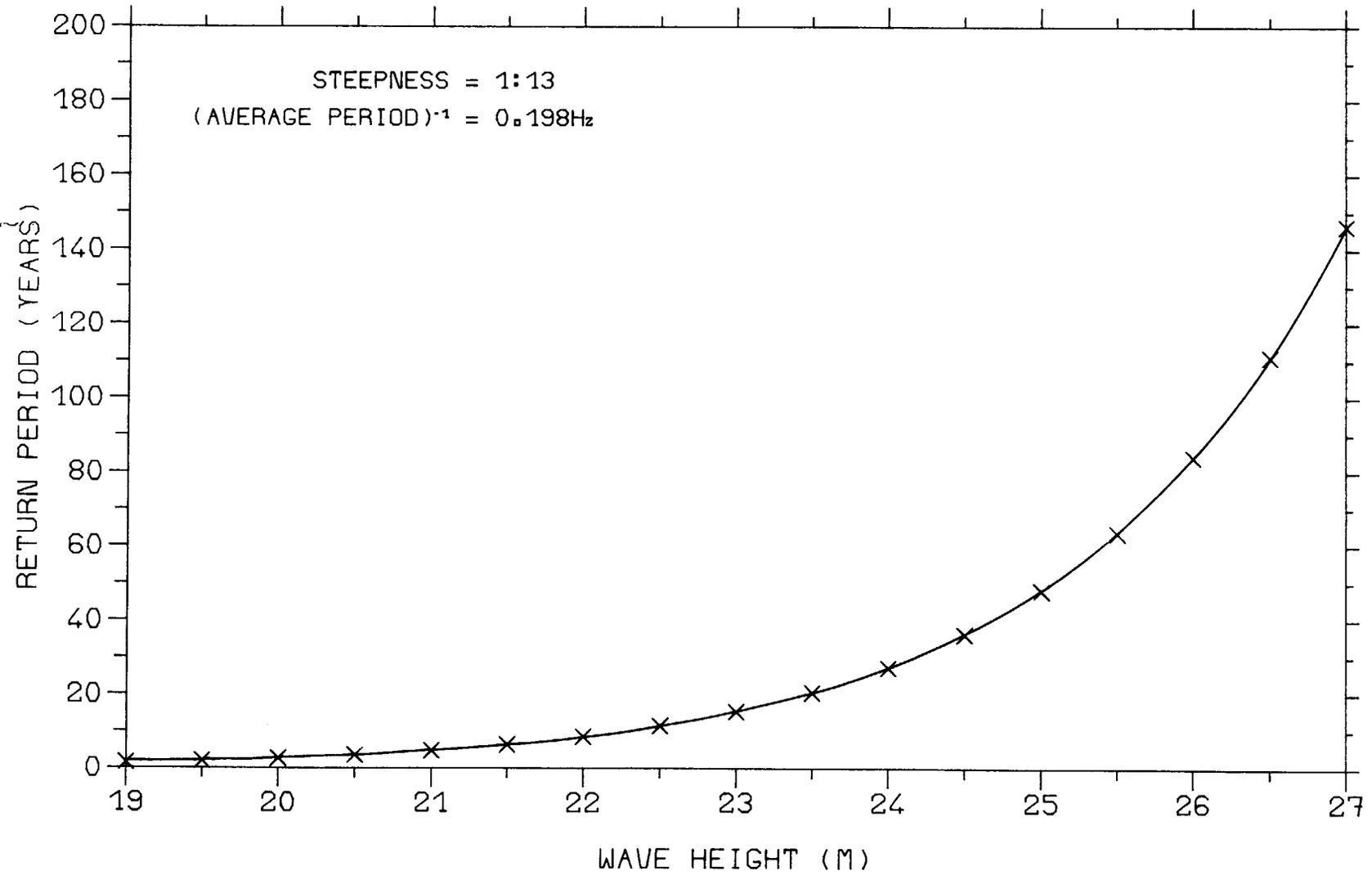

RETURN PERIOD v. WAVE HEIGHT - INDIVIDUAL WAVE MODEL

KINNAIRDS HEAD FEB 1980 - JAN 1982

FIG 3.3.3

KH8082

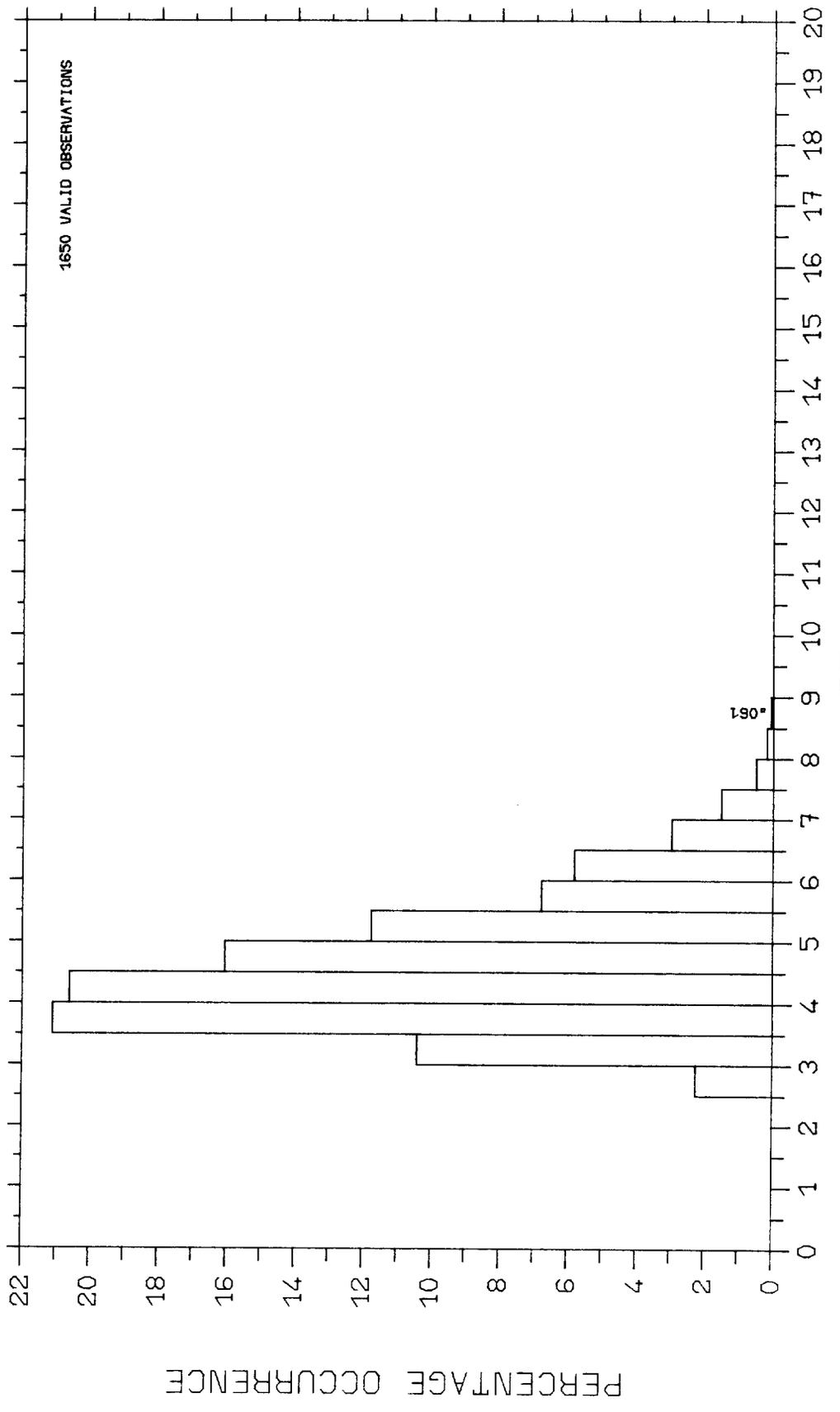

PERCENTAGE OCCURRENCE HISTOGRAM

KINNAIRDS HEAD FEB 1980 - JAN 1982 SUMMERS

FIG 3.4.1.1

KH8082

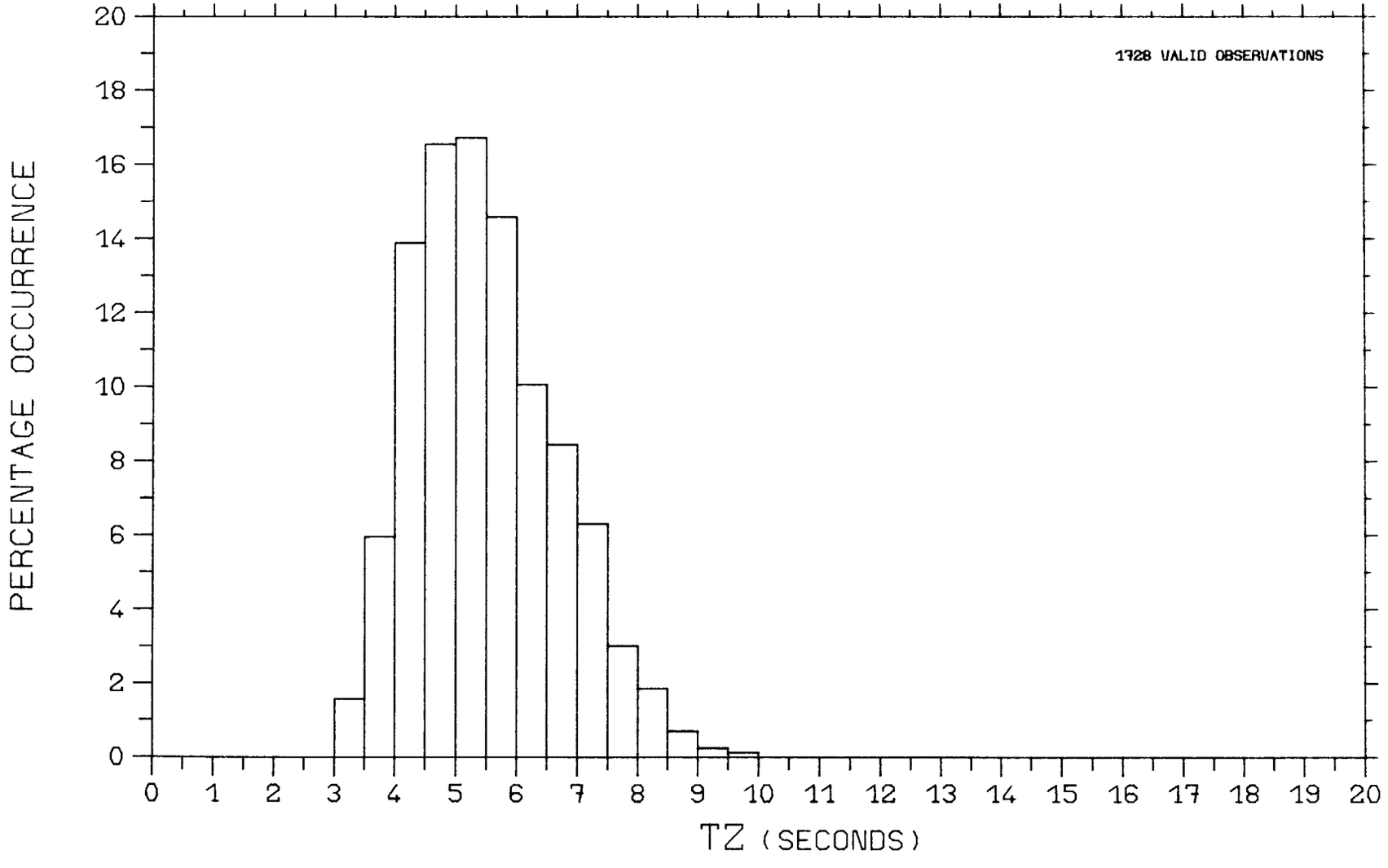

PERCENTAGE OCCURRENCE HISTOGRAM

KINNAIRDS HEAD FEB 1980 - JAN 1982 WINTERS

FIG 3.4.1.2

KH8082

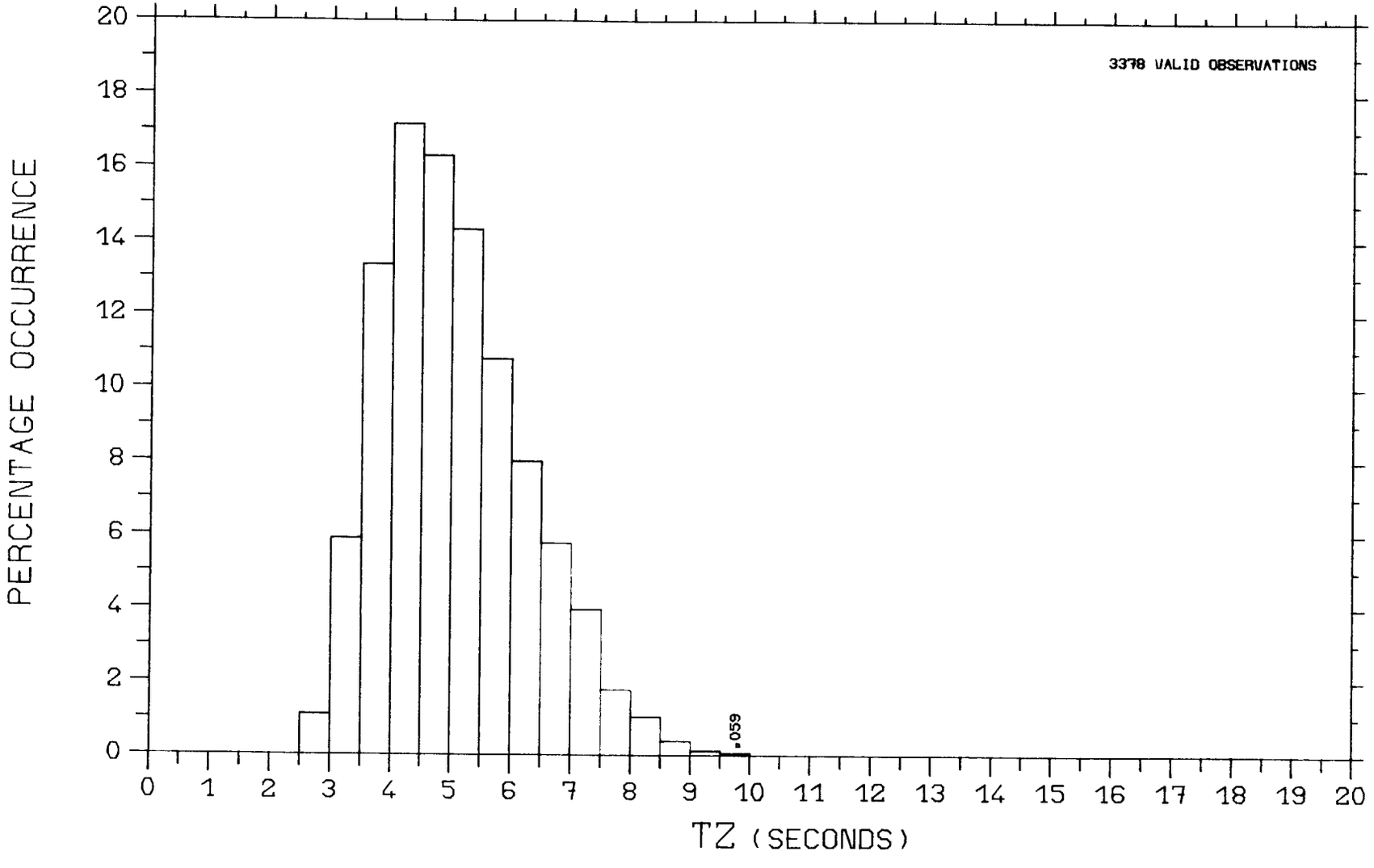

PERCENTAGE OCCURRENCE HISTOGRAM

KINNAIRDS HEAD FEB 1980 - JAN 1982

FIG 3.4.1.3

KH8082

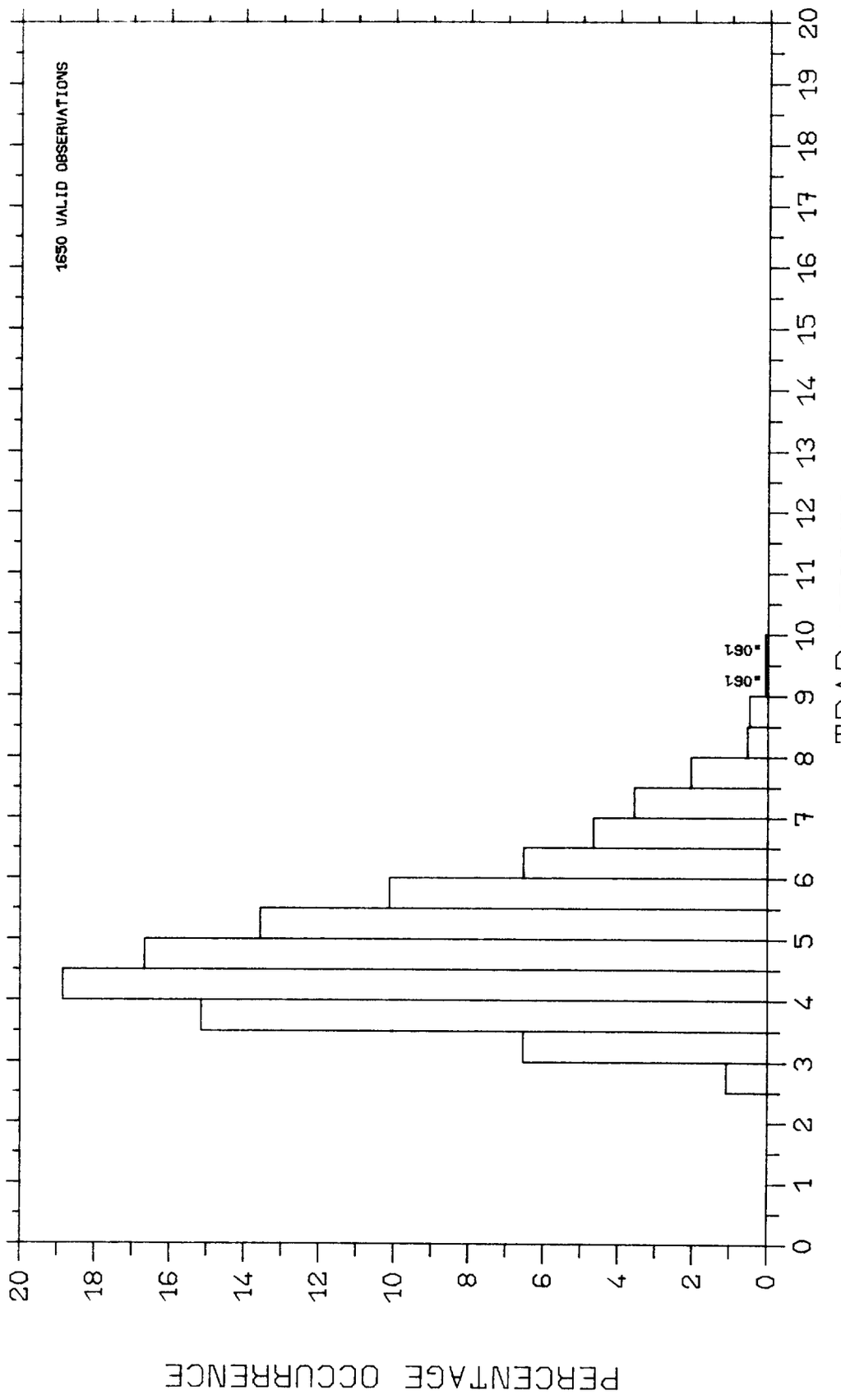

PERCENTAGE OCCURRENCE HISTOGRAM

KINNAIRDS HEAD FEB 1980 - JAN 1982 SUMMERS

FIG 3.4.2.1

KH8082

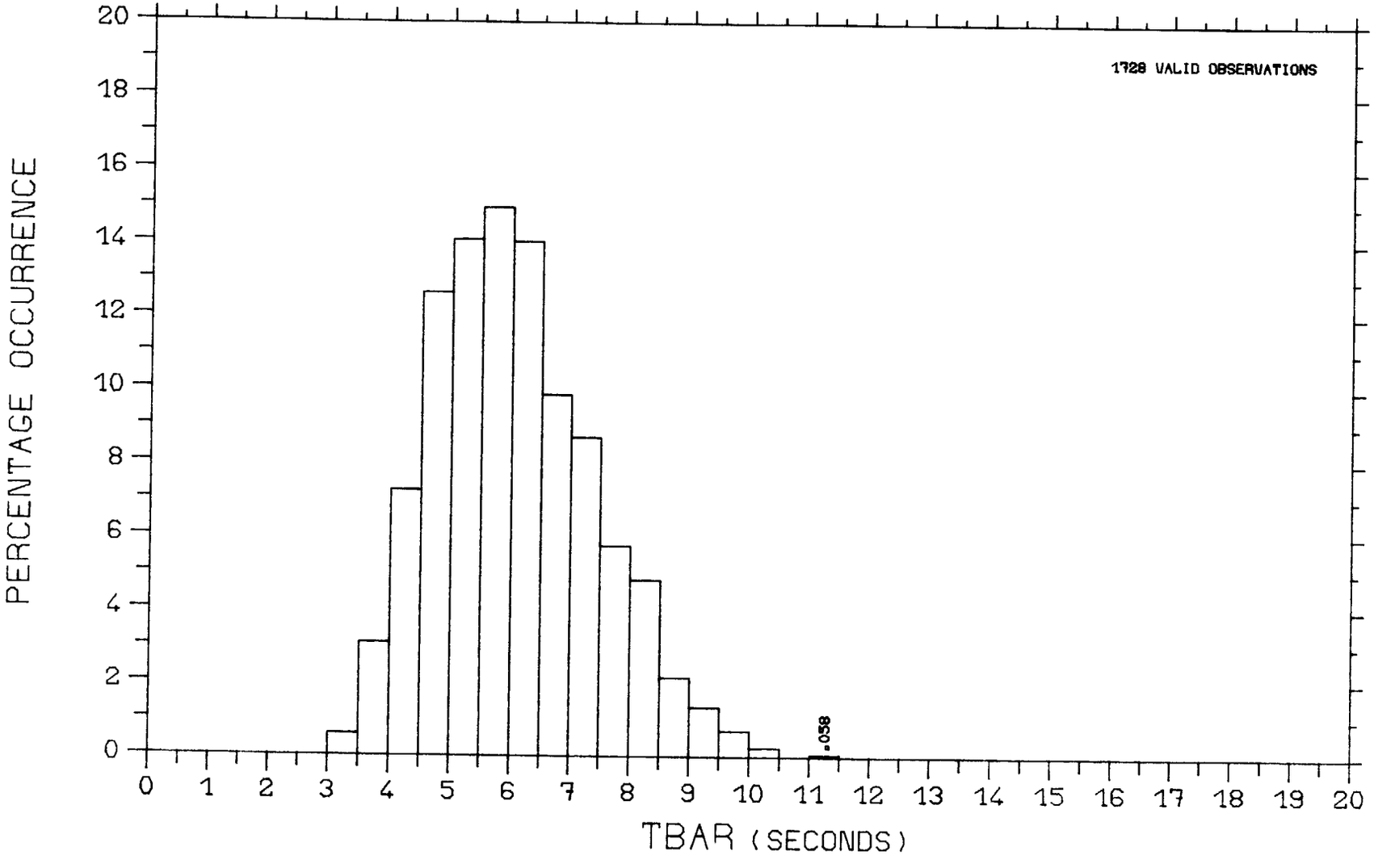

PERCENTAGE OCCURRENCE HISTOGRAM

KINNAIRDS HEAD FEB 1980 - JAN 1982 WINTERS

FIG 3.4.2.2

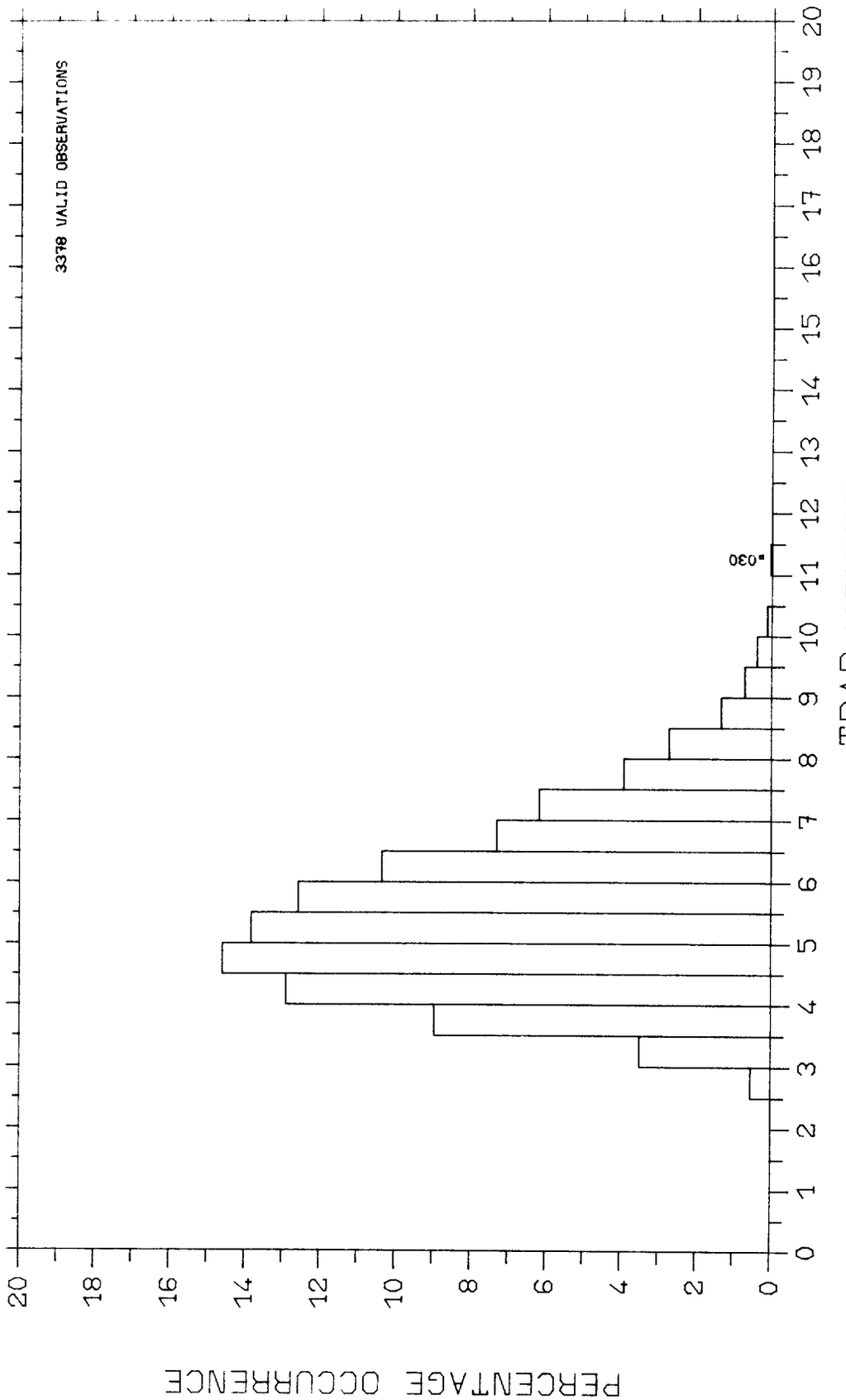

PERCENTAGE OCCURRENCE HISTOGRAM

KINNAIRDS HEAD FEB 1980 - JAN 1982

FIG 3.4.2.3

KH8082

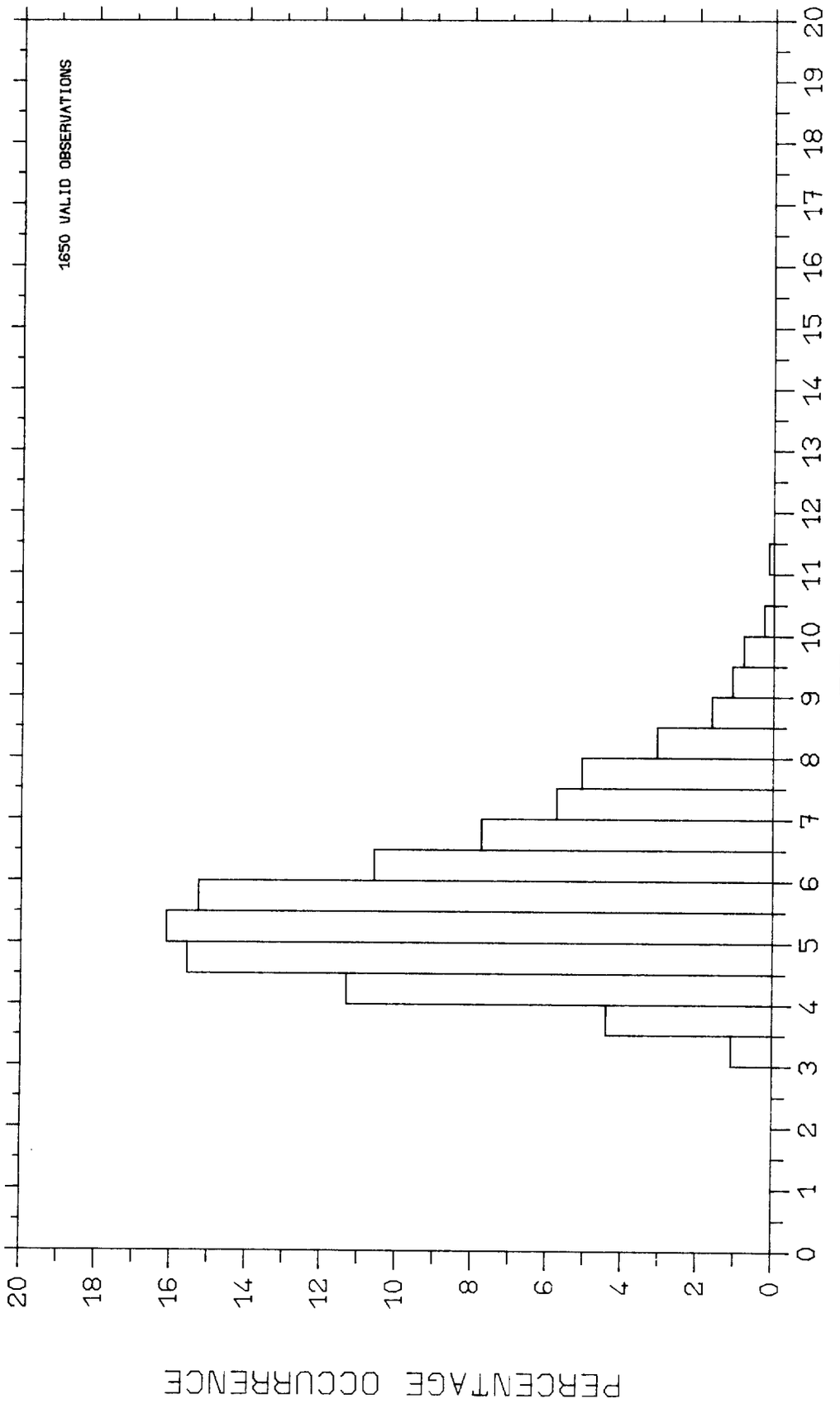

PERCENTAGE OCCURRENCE HISTOGRAM

KINNAIRDS HEAD FEB 1980 - JAN 1982 SUMMERS

FIG 3.4.3.1

KH8082

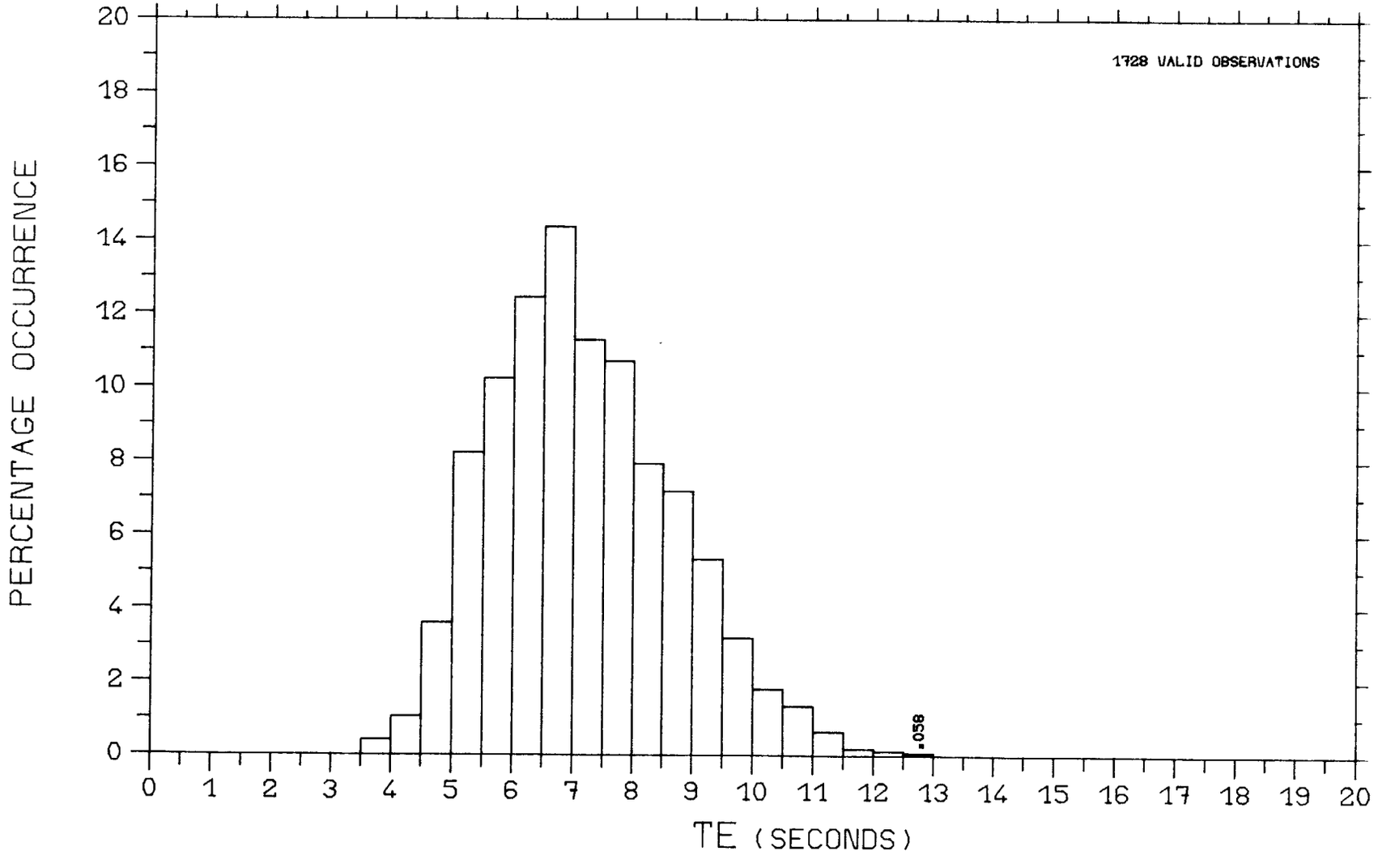

PERCENTAGE OCCURRENCE HISTOGRAM

KINNAIRDS HEAD FEB 1980 - JAN 1982 WINTERS

KH8082

FIG 3.4.3.2

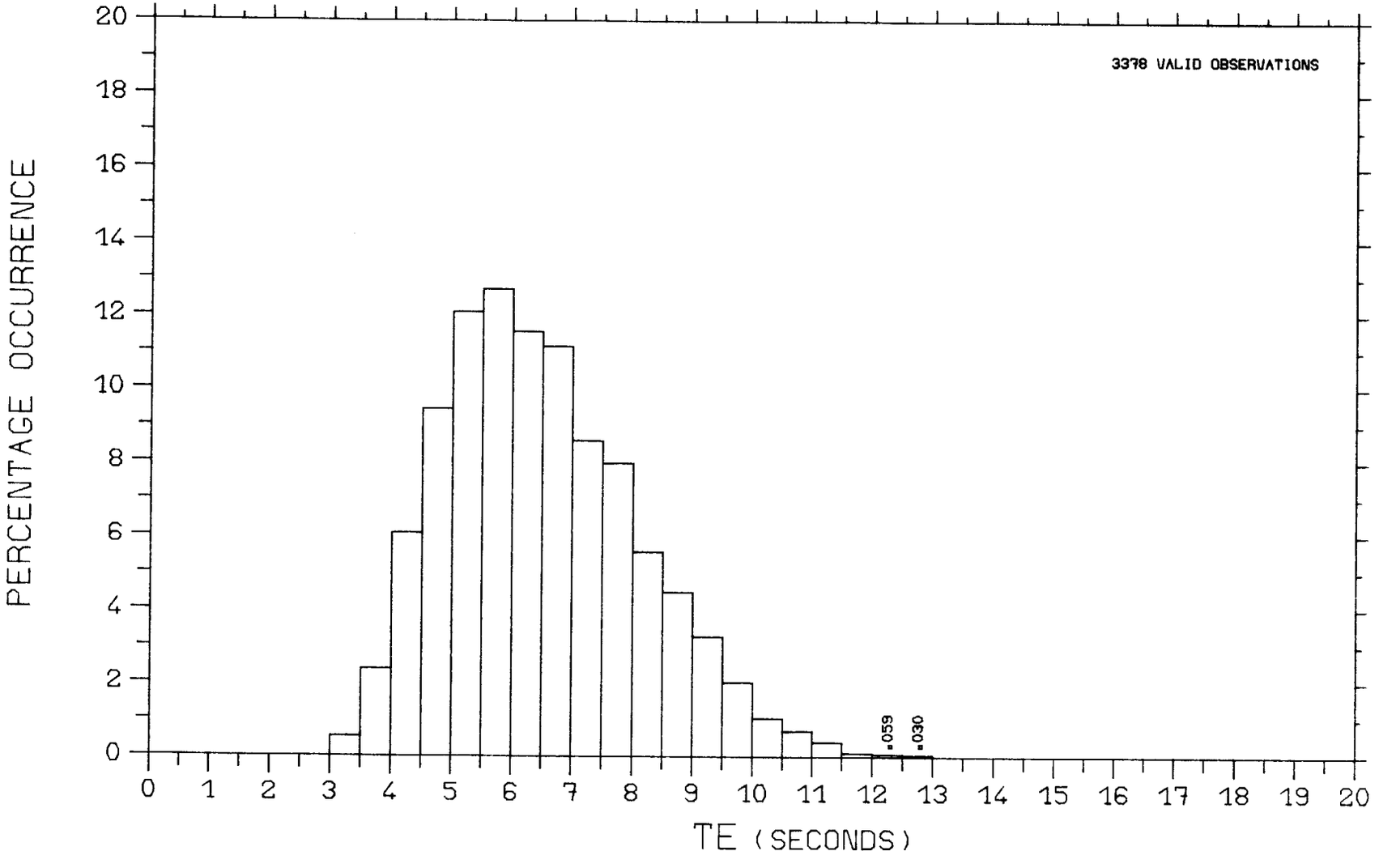

PERCENTAGE OCCURRENCE HISTOGRAM

KINNAIRDS HEAD FEB 1980 - JAN 1982

KH8082

FIG 3.4.3.3

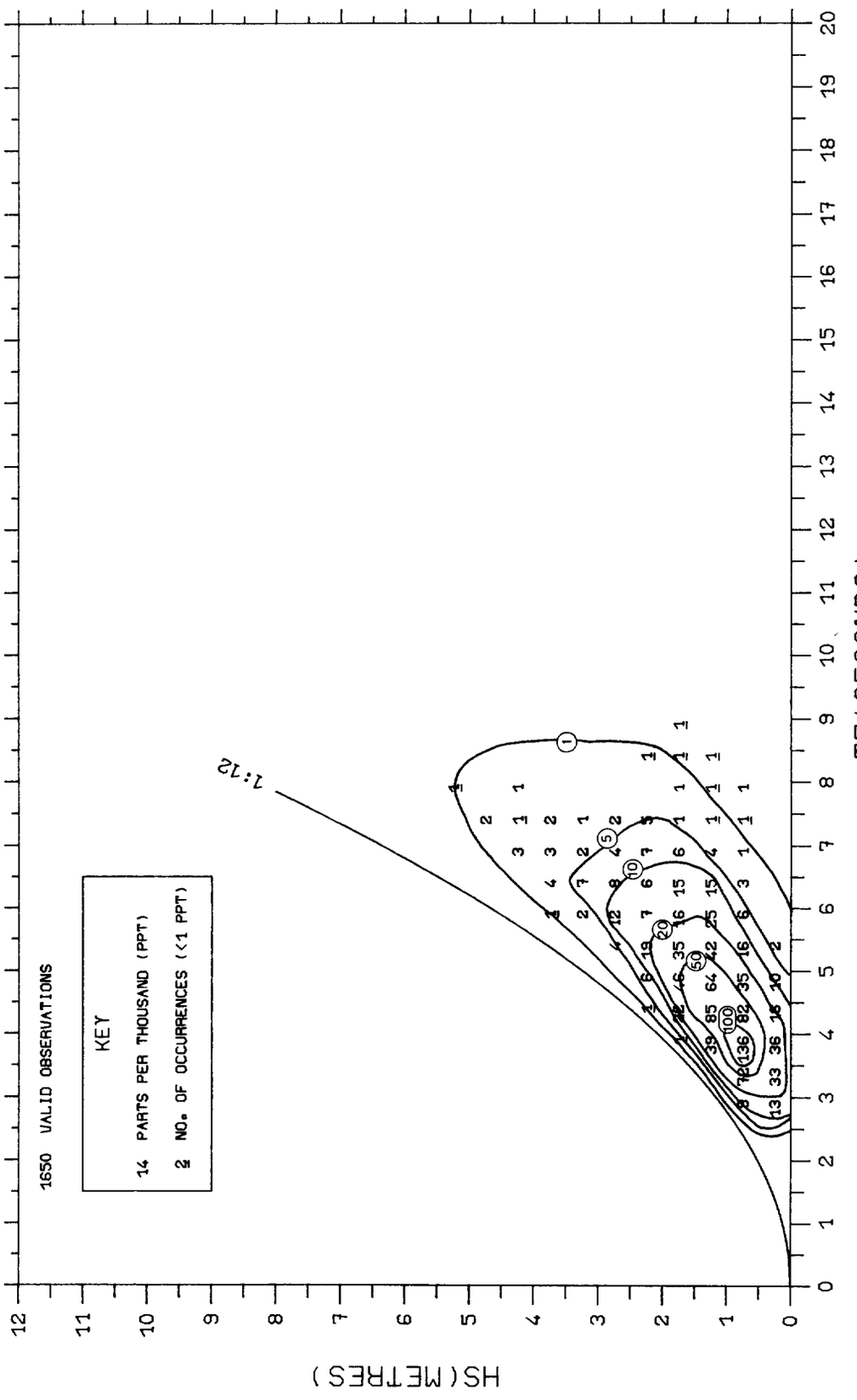

SCATTER PLOT OF HS AND TZ

KINNAIRDS HEAD FEB 1980 - JAN 1982 SUMMERS

FIG 3.5.1.1

KH8082

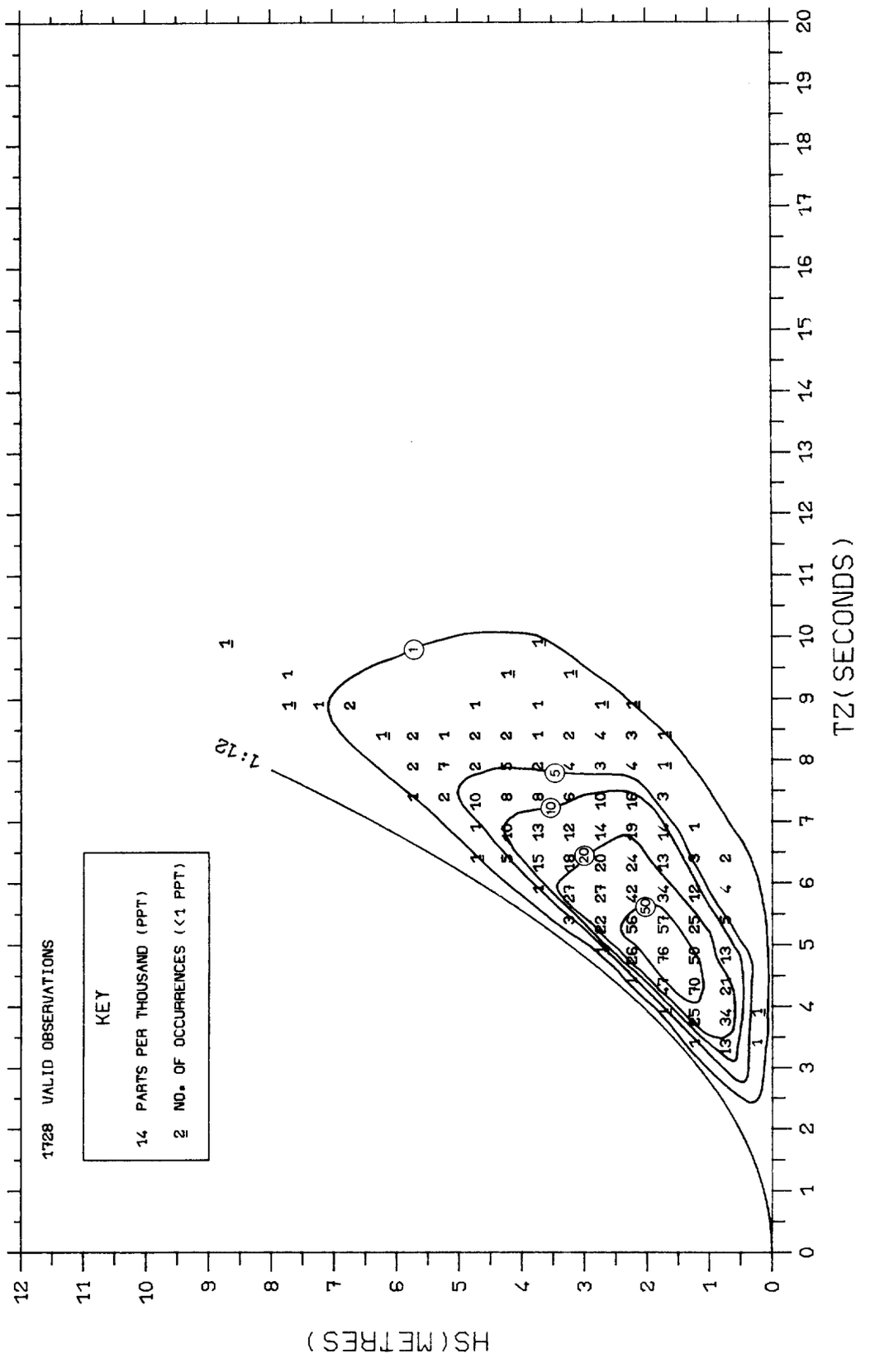

SCATTER PLOT OF HS AND TZ

KINNAIRDS HEAD FEB 1980 - JAN 1982 WINTERS

FIG 3.5.1.2

KH8082

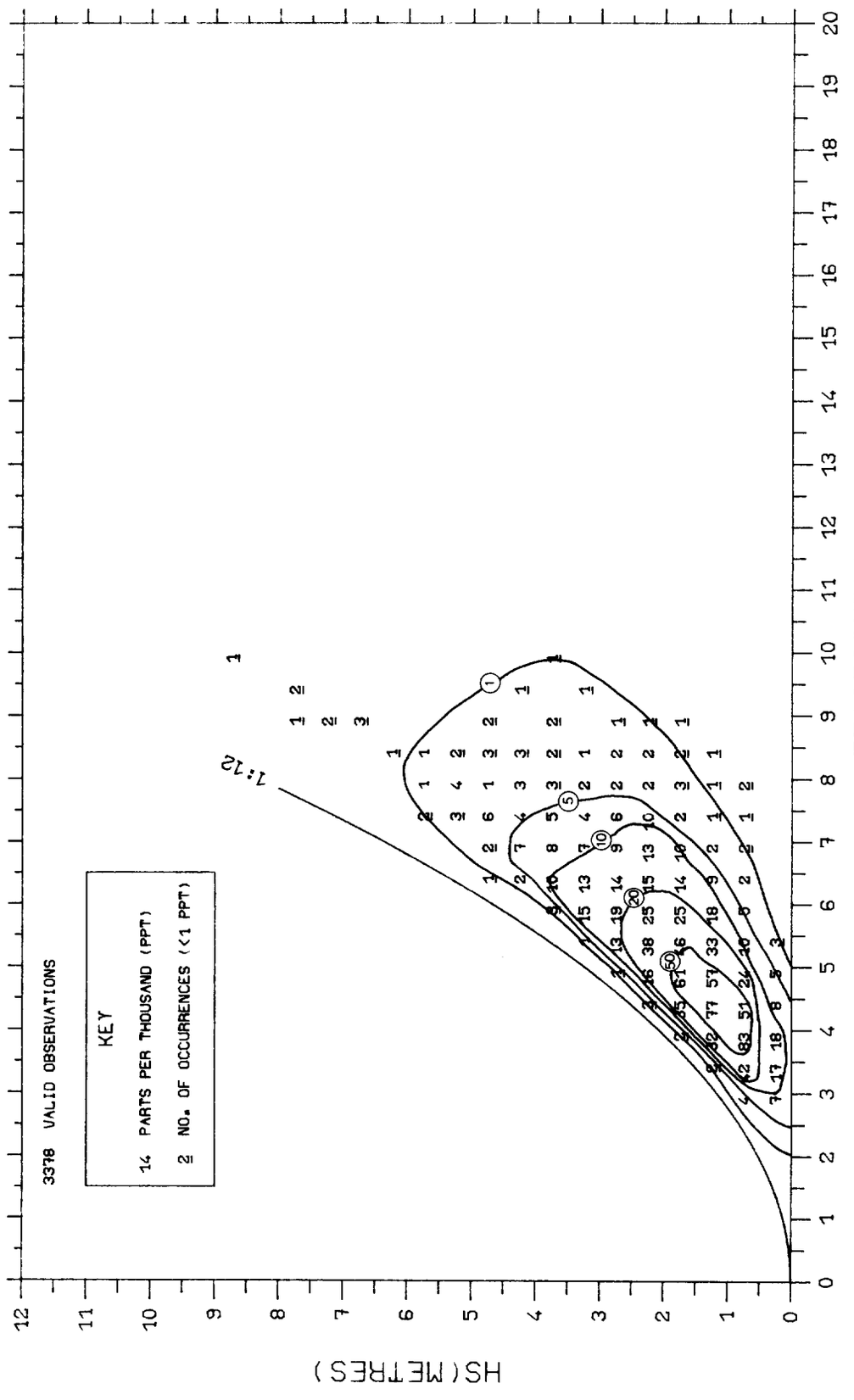

SCATTER PLOT OF HS AND TZ

KINNAIRDS HEAD FEB 1980 - JAN 1982

FIG 3.5.1.3

KH8082

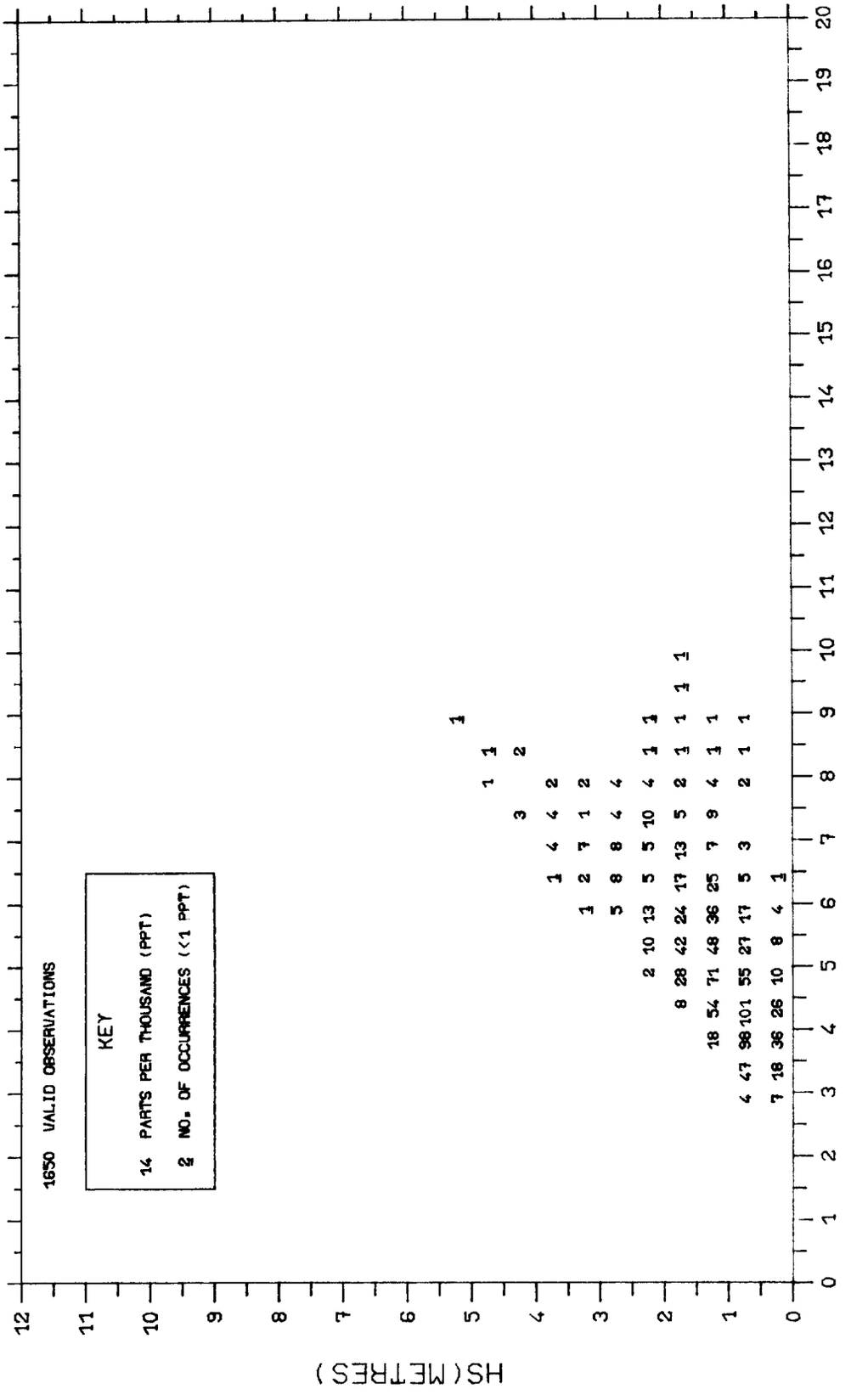

SCATTER PLOT OF HS AND TBAR

KINNAIRDS HEAD FEB 1980 - JAN 1982 SUMMERS

FIG 3.5.2.1

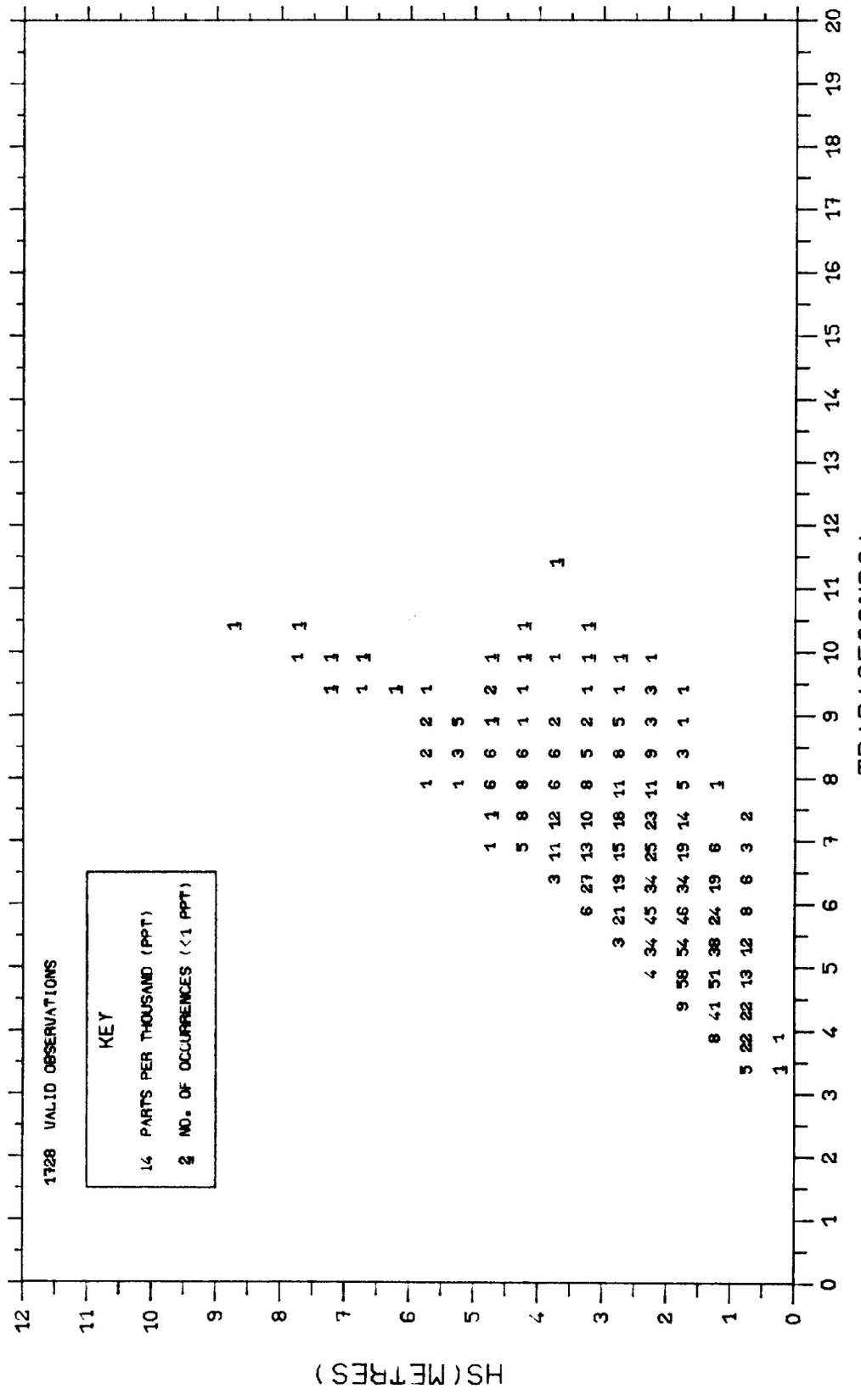

SCATTER PLOT OF HS AND TBAR

KINNAIRDS HEAD FEB 1980 - JAN 1982 WINTERS

FIG 3.5.2.2

KH8082

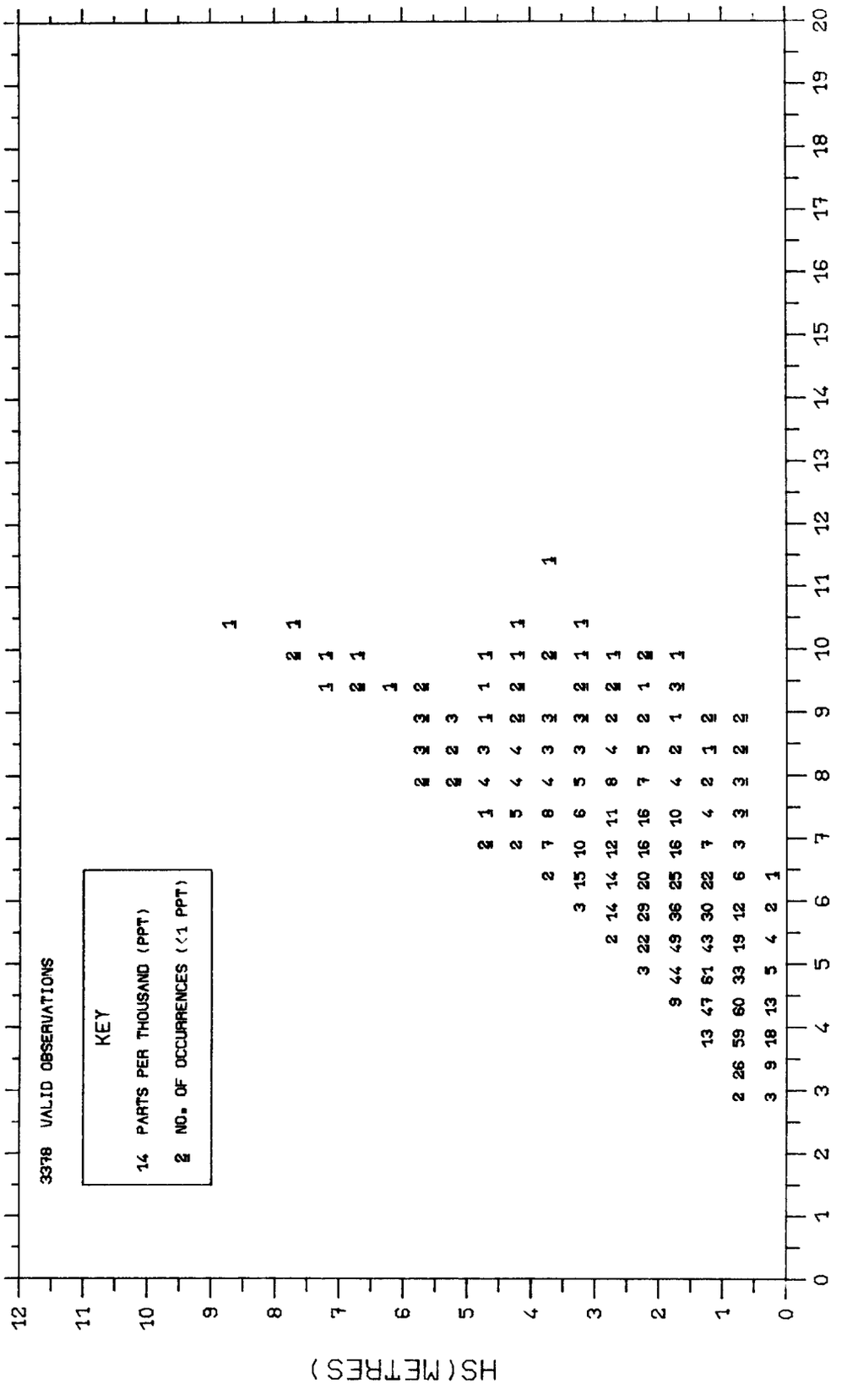

SCATTER PLOT OF HS AND TBAR

KINNAIRDS HEAD FEB 1980 - JAN 1982

FIG 3.5.2.3

KH8082

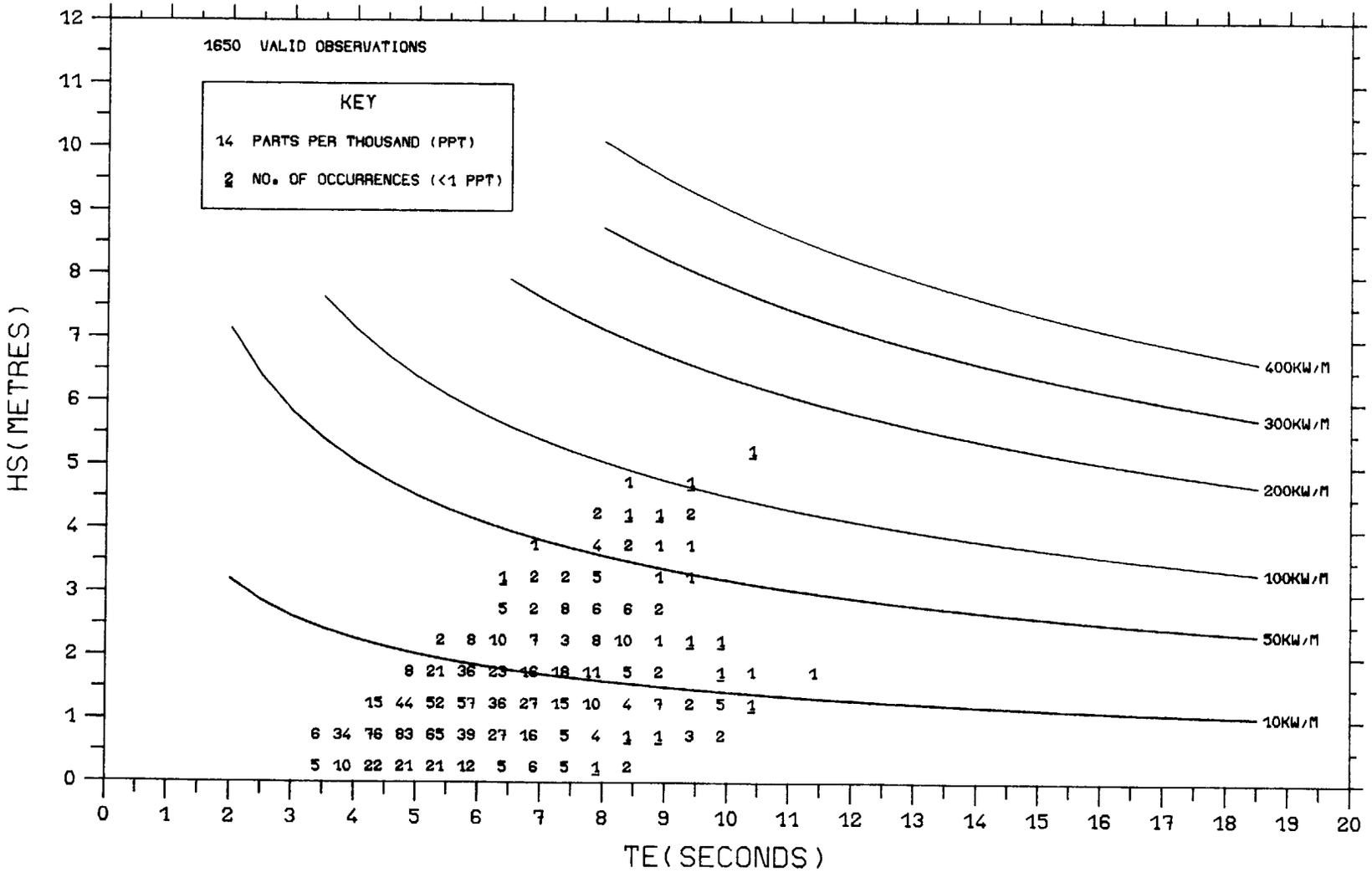

SCATTER PLOT OF HS AND TE

KINNAIRDS HEAD FEB 1980 - JAN 1982 SUMMERS

KH8082

FIG 3.5.3.1

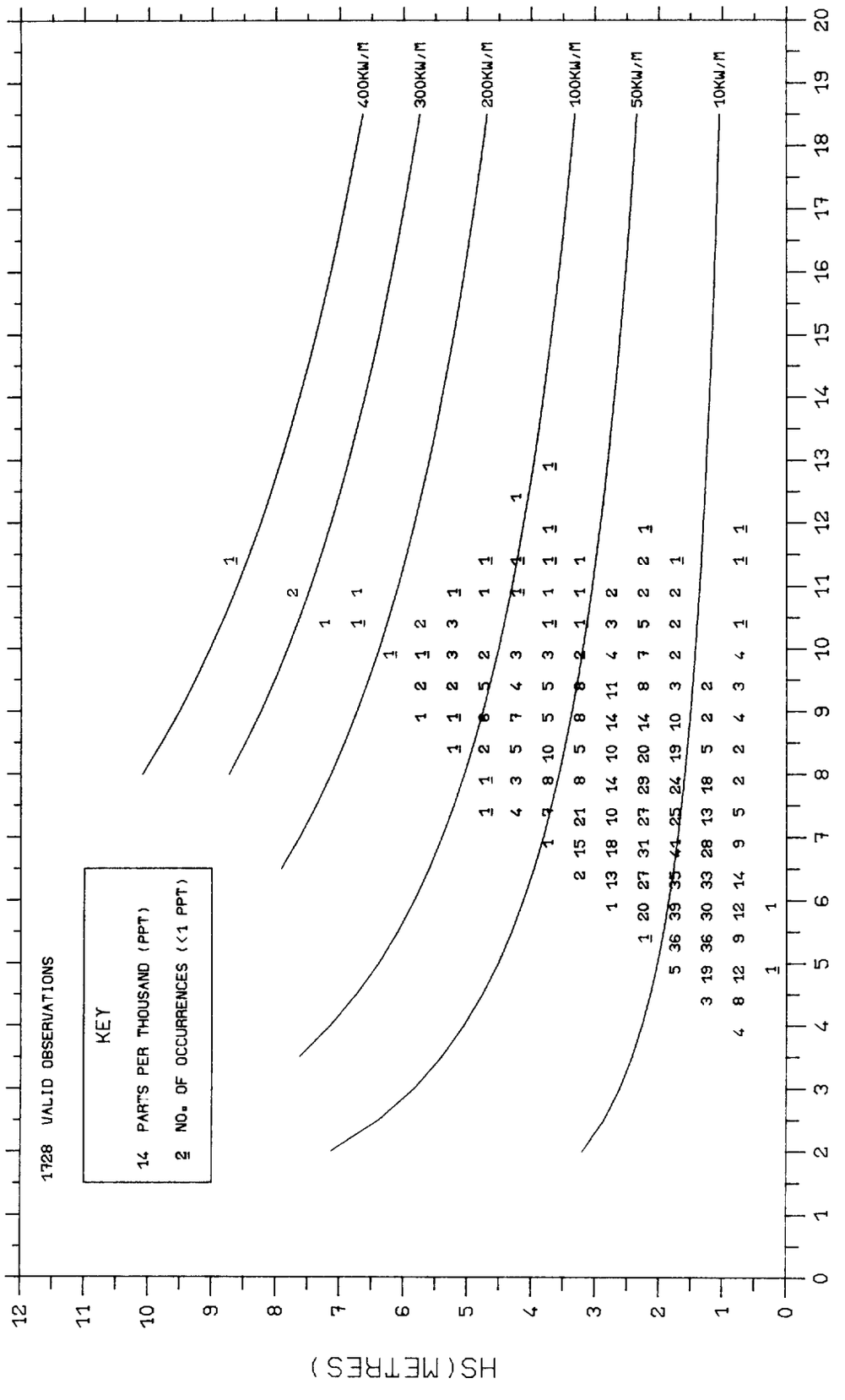

SCATTER PLOT OF HS AND TE

KINNAIRDS HEAD FEB 1980 - JAN 1982 WINTERS

FIG 3.5.3.2

KH8082

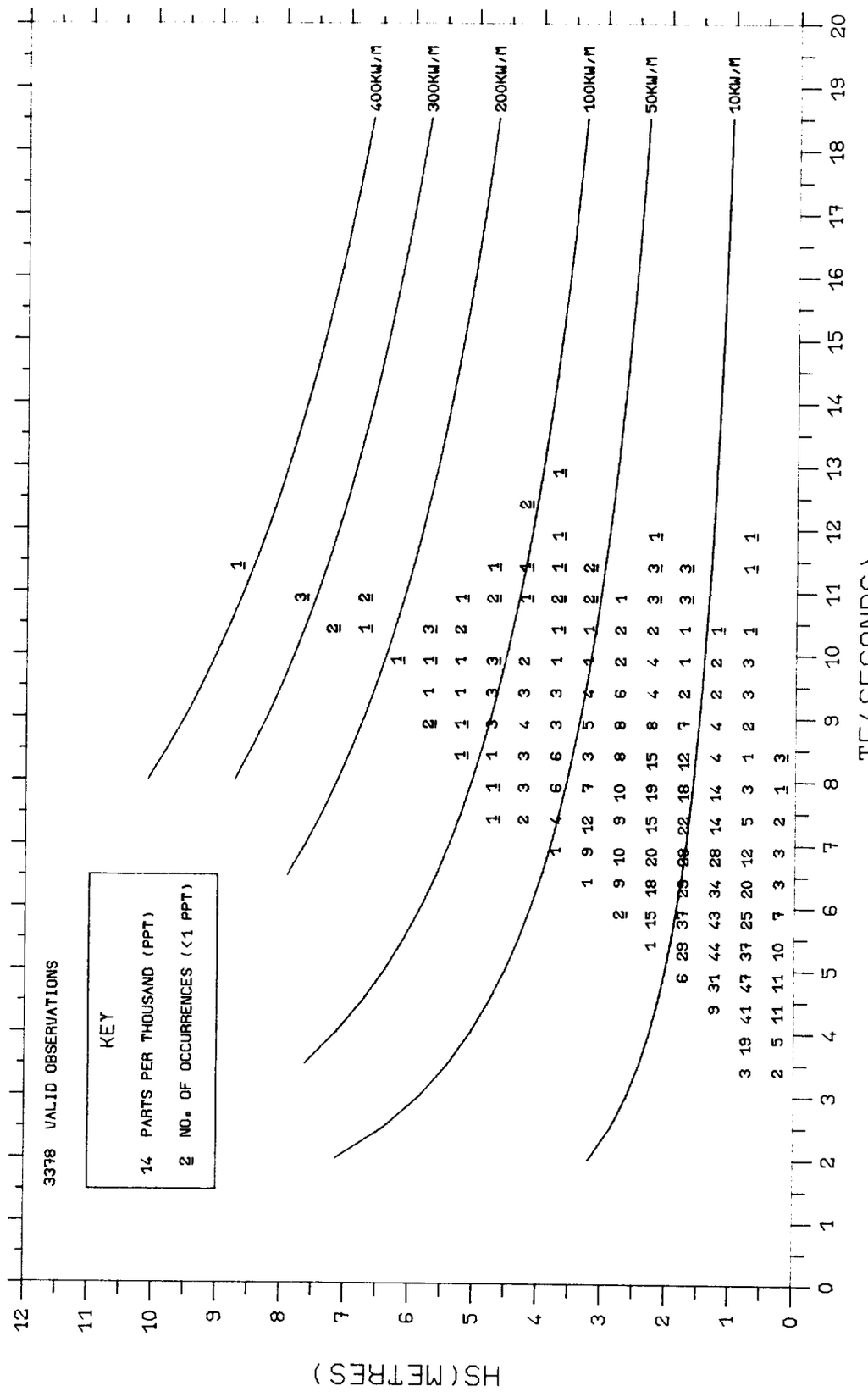

SCATTER PLOT OF HS AND TE

KINNAIRDS HEAD FEB 1980 - JAN 1982

FIG 3.5.3.3

KH8082

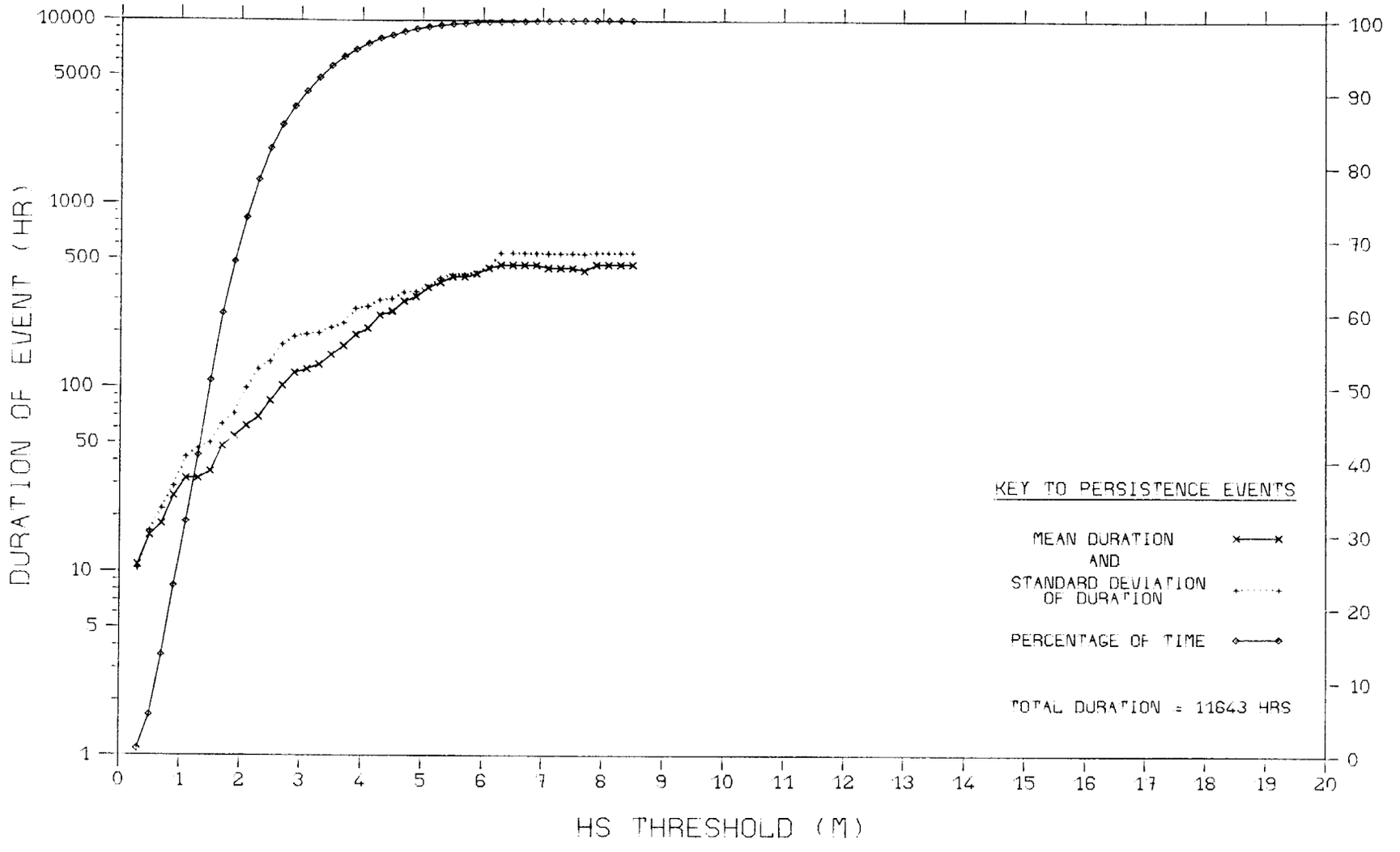

KINNAIRDS HEAD FEB 1980 - JAN 1982

CALMS

FIG 3.6.1

KH8082

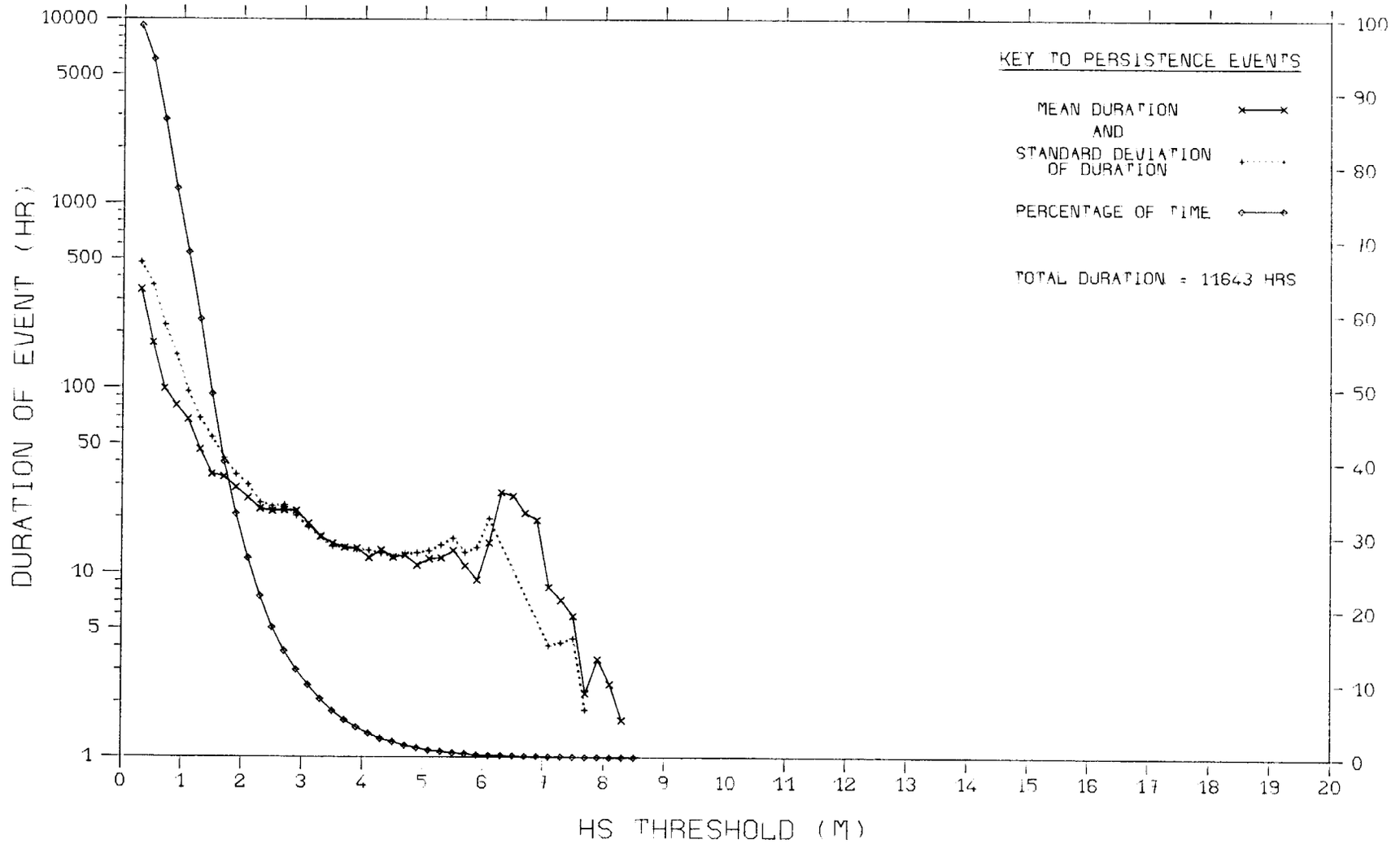

KINNAIRDS HEAD FEB 1980 - JAN 1982

STORMS

FIG 3.6.2

KH8082

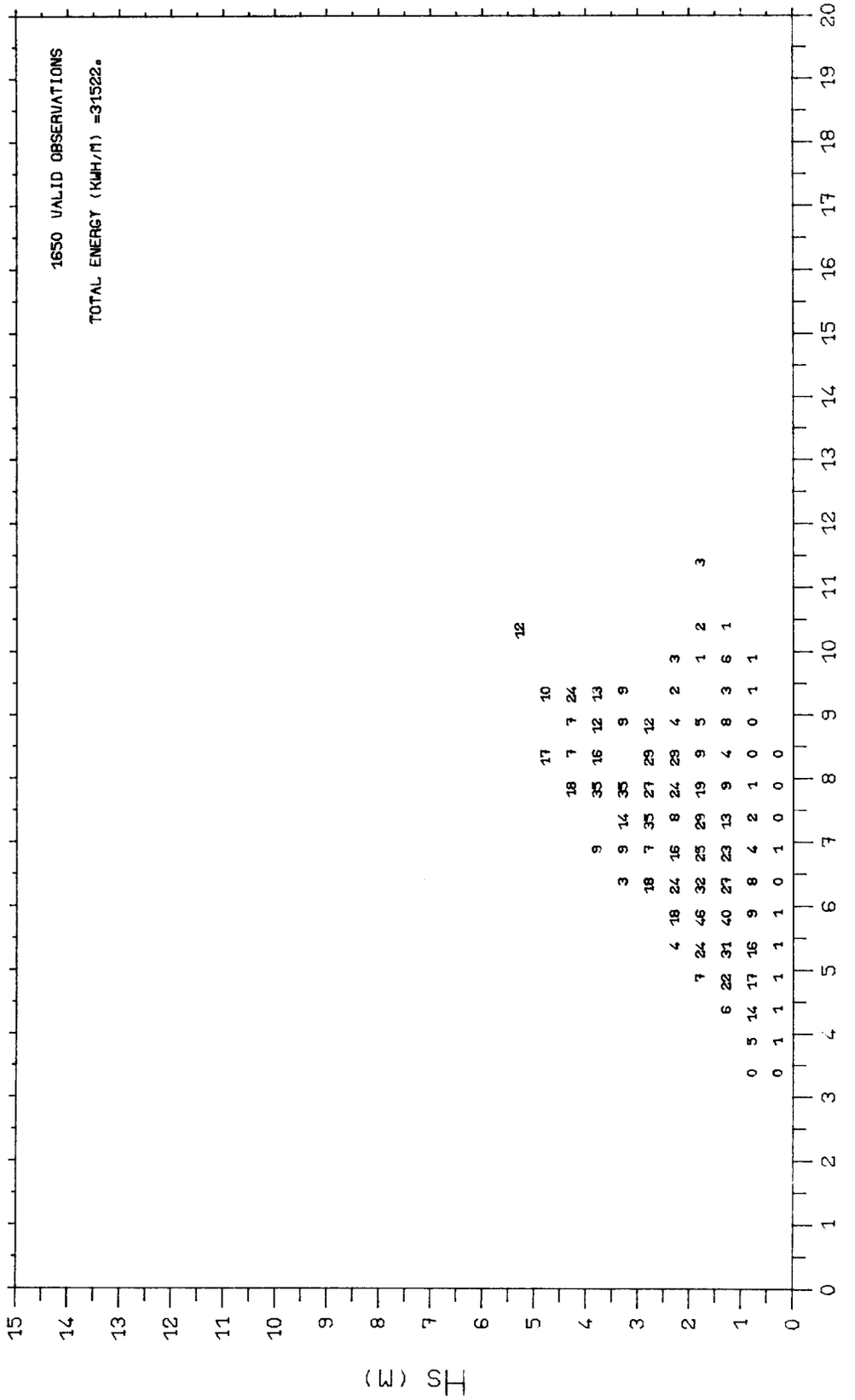

DISTRIBUTION OF TOTAL MEASURED WAVE ENERGY

WITH H_S AND T_E (PPT)

KINNAIRDS HEAD FEB 1980 - JAN 1982 SUMMERS

FIG 3.7.1

KH8082

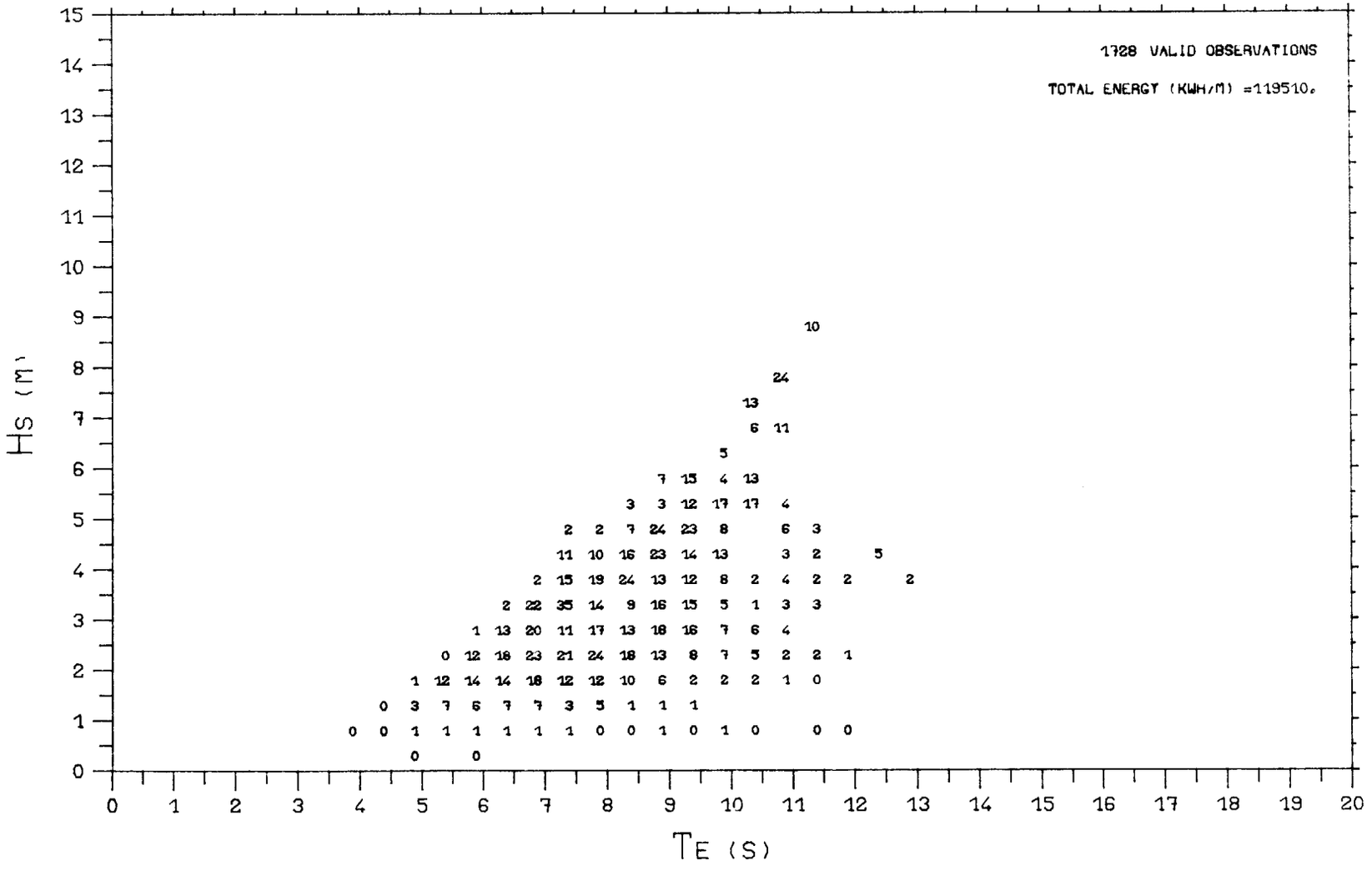

DISTRIBUTION OF TOTAL MEASURED WAVE ENERGY
WITH Hs AND TE (PPT)

KINNAIRDS HEAD FEB 19ε) - JAN 1982 WINTERS

FIG 3.7.2

KH8082

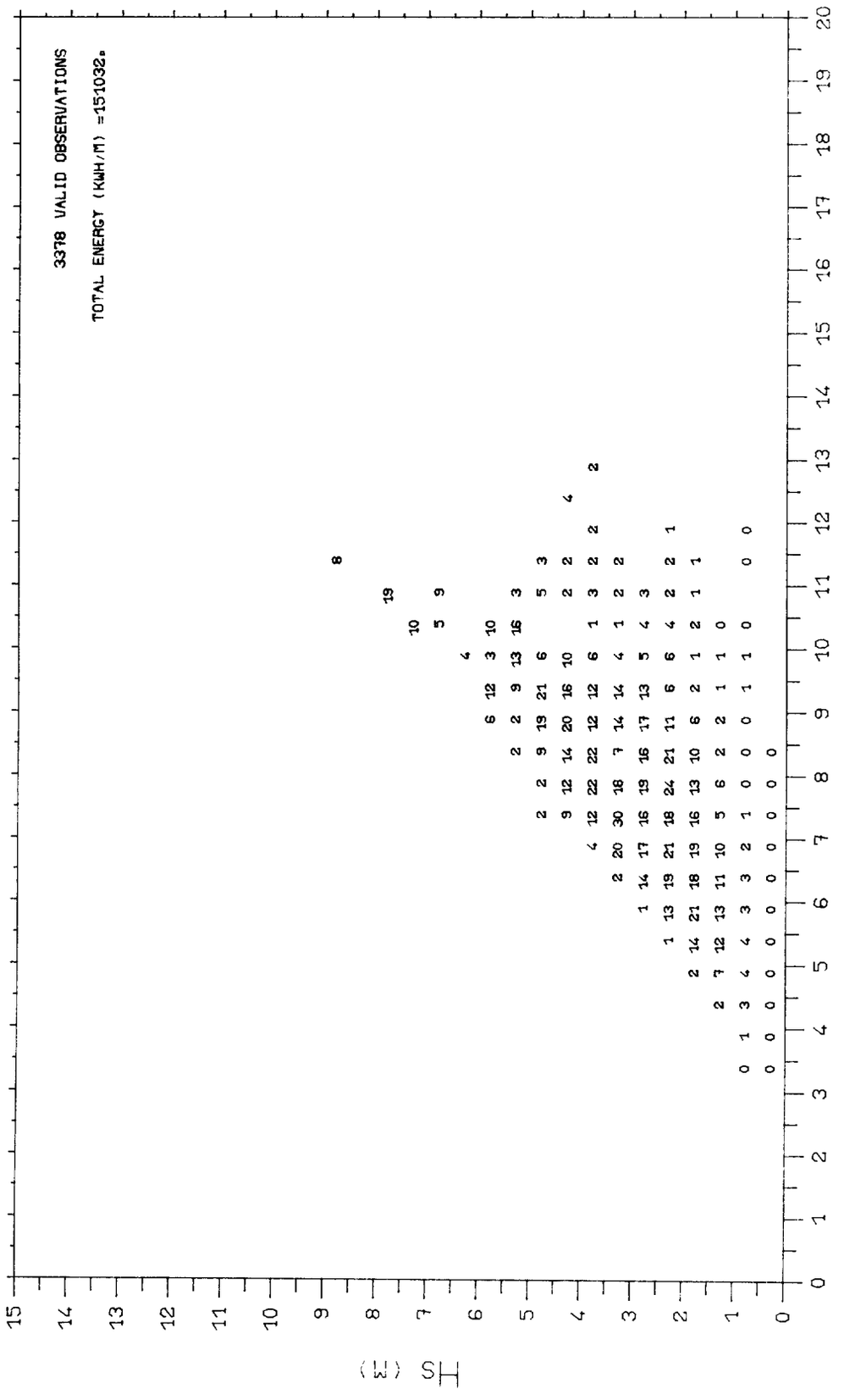

DISTRIBUTION OF TOTAL MEASURED WAVE ENERGY
WITH H_S AND T_E (PPT)

KINNAIRDS HEAD FEB 1980 - JAN 1982

FIG 3.7.3

KH8082

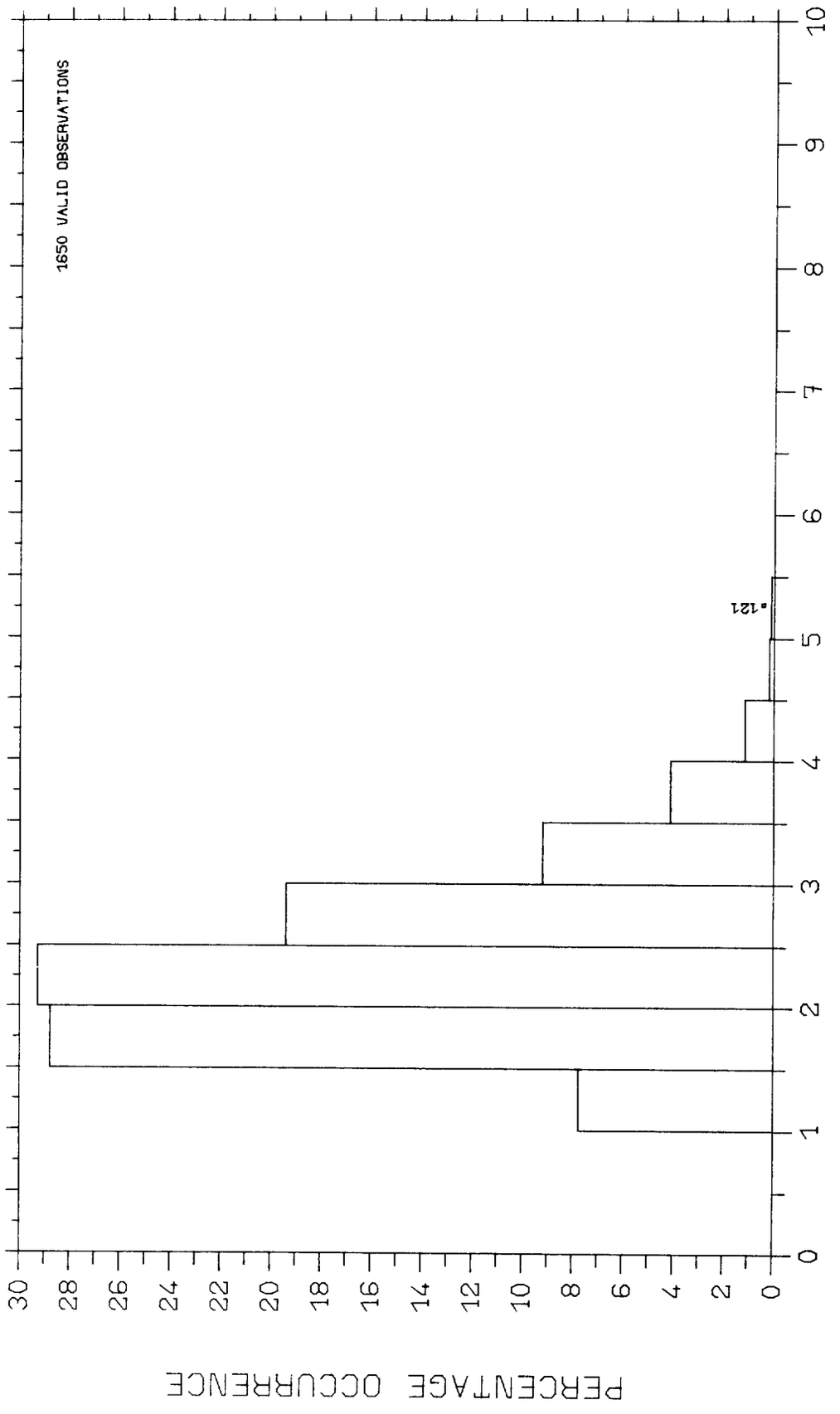

PERCENTAGE OCCURRENCE HISTOGRAM

KINNAIRDS HEAD FEB 1980 - JAN 1982 SUMMERS

FIG 3.8.1

KH8082

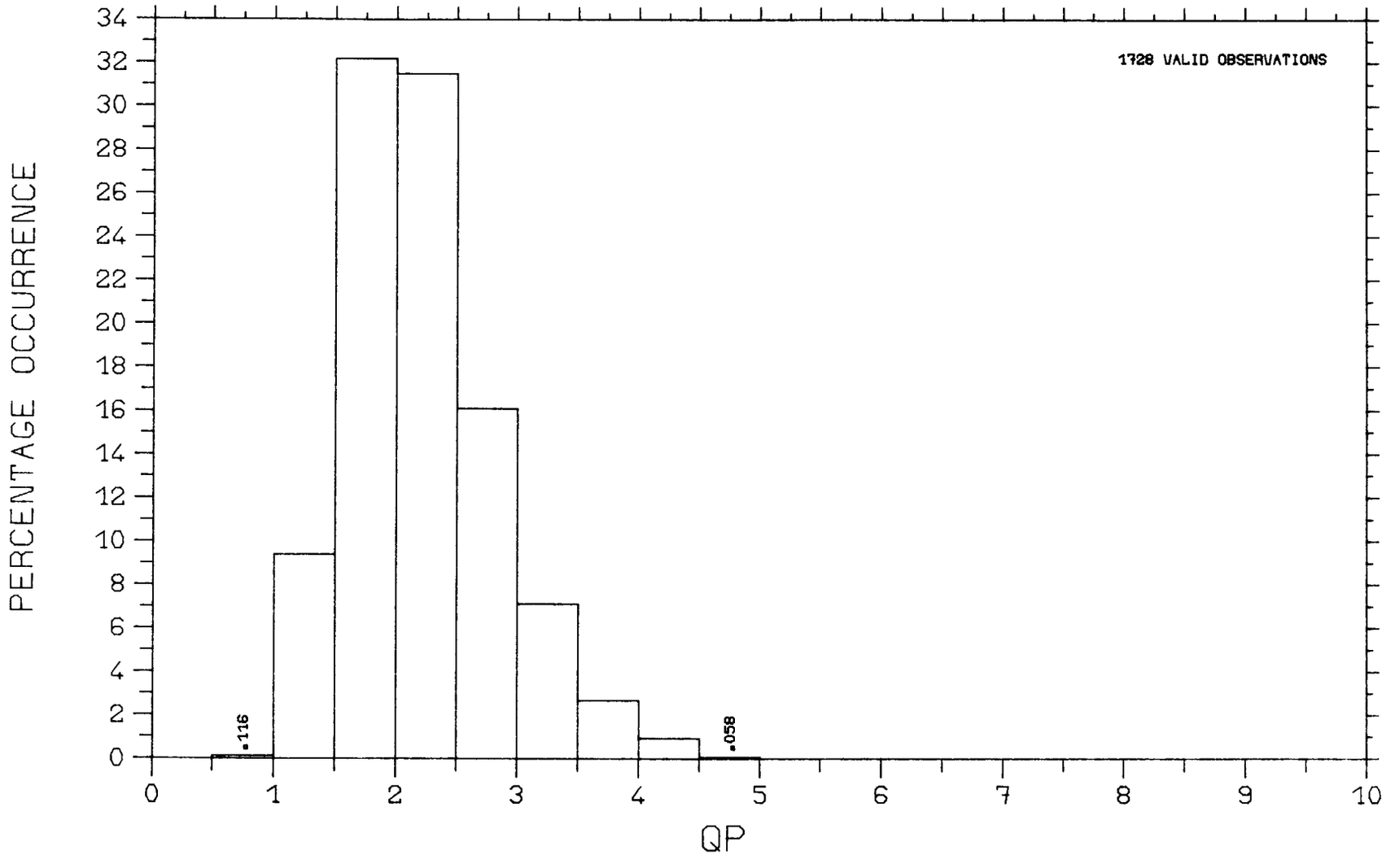

PERCENTAGE OCCURRENCE HISTOGRAM

KINNAIRDS HEAD FEB 1980 - JAN 1982 WINTERS

FIG 3.8.2

KH8082

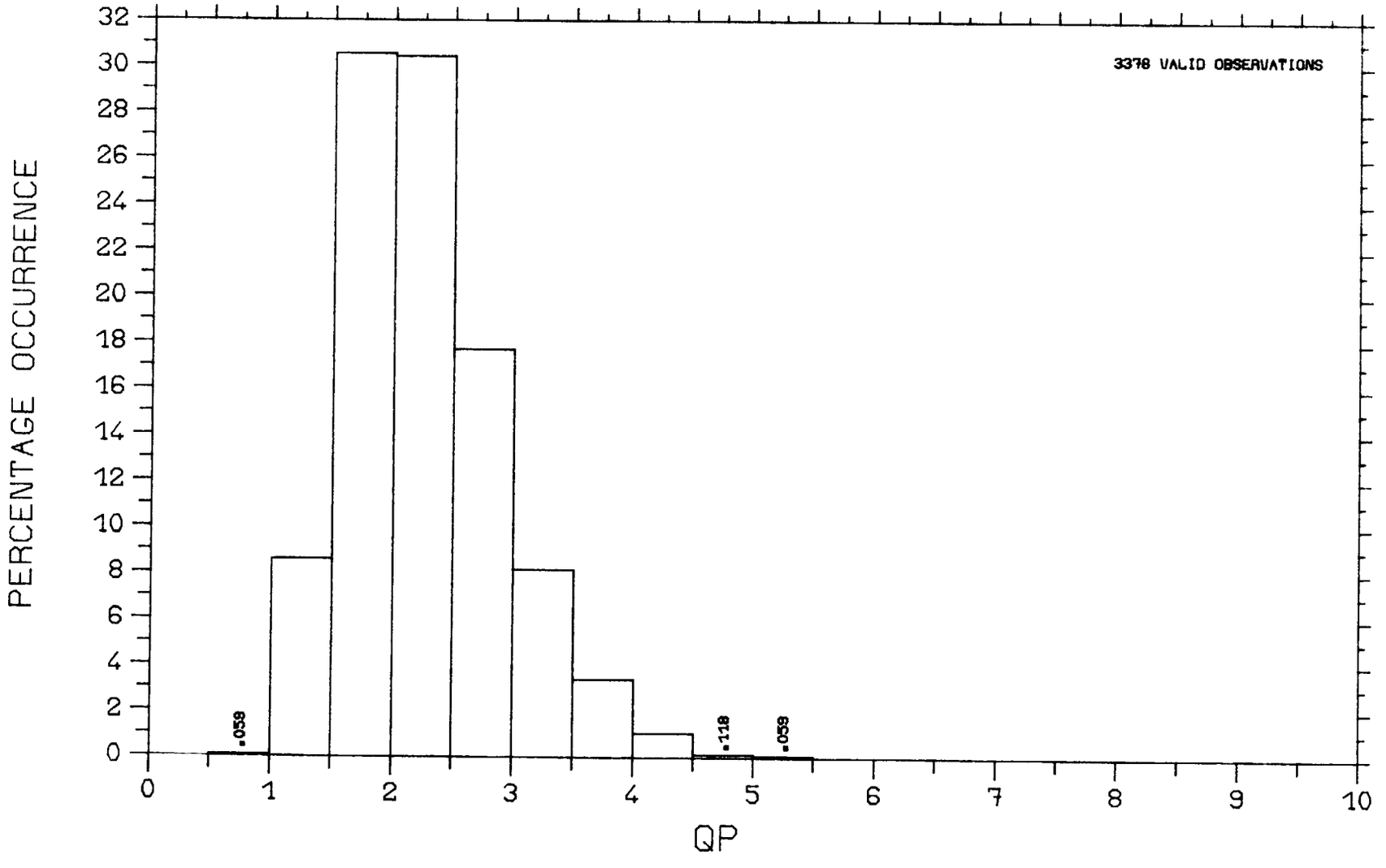

PERCENTAGE OCCURRENCE HISTOGRAM

KINNAIRDS HEAD FEB 1980 - JAN 1982

FIG 3.8.3

KH8082